JOURNAL OF GEOPHYSICAL RESEARCH, VOL. 111, D22214, doi:10.1029/2006JD007216, 2006

Pan-Arctic enhancements of light absorbing aerosol concentrations due to North American boreal forest fires during summer 2004

A. Stohl,[1] E. Andrews,[2,3] J. F. Burkhart,[4] C. Forster,[1] A. Herber,[5] S. W. Hoch,[6] D. Kowal,[7] C. Lunder,[1] T. Mefford,[2,3] J. A. Ogren,[2] S. Sharma,[8] N. Spichtinger,[9] K. Stebel,[1] R. Stone,[2,3] J. Ström,[10] K. Tørseth,[1] C. Wehrli,[11] and K. E. Yttri[1]

Received 20 February 2006; revised 27 July 2006; accepted 9 August 2006; published 23 November 2006.

[1] During summer of 2004, about 2.7 million hectare of boreal forest burned in Alaska, the largest annual area burned on record, and another 3.1 million hectare burned in Canada. This study explores the impact of emissions from these fires on light absorbing aerosol concentration levels, aerosol optical depths (AOD), and albedo at the Arctic stations Barrow (Alaska), Alert (Canada), Summit (Greenland), and Zeppelin/Ny Ålesund on Spitsbergen (Norway). The Lagrangian particle dispersion model FLEXPART was run backward from these sites to identify periods that were influenced by forest fire pollution plumes. It is shown that the fires led to enhanced values of particle light absorption coefficients (σ_{ap}) at all of these sites. Barrow, about 1000 km away from the fires, was affected by several fire pollution plumes, one leading to spectacularly high 3-hour mean σ_{ap} values of up to 32 Mm^{-1}, more than the highest values measured in Arctic Haze. AOD measurements for a wavelength of 500 nm saturated but were estimated at above 4–5 units, unprecedented in the station records. Fire plumes were transported through the atmospheric column over Summit continuously for 2 months, during which all measured AOD values were enhanced, with maxima up to 0.4–0.5 units. Equivalent black carbon concentrations at the surface at Summit were up to 600 ng m^{-3} during two major episodes, and Alert saw at least one event with enhanced σ_{ap} values. FLEXPART results show that Zeppelin was located in a relatively unaffected part of the Arctic. Nevertheless, there was a 4-day period with daily mean $\sigma_{ap} > 0.3$ Mm^{-1}, the strongest episode of the summer half year, and enhanced AOD values. Elevated concentrations of the highly source-specific compound levoglucosan positively confirmed that biomass burning was the source of the aerosols at Zeppelin. In summary, this paper shows that boreal forest fires can lead to elevated concentrations of light absorbing aerosols throughout the entire Arctic. Enhanced AOD values suggest a substantial impact of these plumes on radiation transmission in the Arctic atmosphere. During the passage of the largest fire plume, a pronounced drop of the albedo of the snow was observed at Summit. We suggest that this is due to the deposition of light absorbing particles on the snow, with further potentially important consequences for the Arctic radiation budget.

Citation: Stohl, A., et al. (2006), Pan-Arctic enhancements of light absorbing aerosol concentrations due to North American boreal forest fires during summer 2004, *J. Geophys. Res.*, *111*, D22214, doi:10.1029/2006JD007216.

1. Introduction

[2] Black carbon (BC) particles are a significant factor in the climate system because of their absorption of light in the atmosphere [*Bond and Bergstrom*, 2005]. In the

[1]Norwegian Institute for Air Research, Kjeller, Norway.
[2]Global Monitoring Division, Earth System Research Laboratory, NOAA, Boulder, Colorado, USA.
[3]Also at Cooperative Institute for Research in Environmental Sciences, University of Colorado, Boulder, Colorado, USA.
[4]School of Engineering, University of California, Merced, California, USA.
[5]Alfred Wegener Institute, Bremerhaven, Germany.
[6]Institute for Atmospheric and Climate Science, Eidgenössische Technische Hochschule, Zurich, Switzerland.
[7]National Geophysical Data Center, NOAA, Boulder, Colorado, USA.
[8]Environment Canada, Toronto, Ontario, Canada.
[9]Wissenschaftszentrum Weihenstephan, Technical University of Munich, Munich, Germany.
[10]Department of Applied Environmental Science, Stockholm University, Stockholm, Sweden.
[11]Physical-Meteorological Observatory, Davos, Switzerland.

0148-0227/06/2006JD007216$09.00

Arctic, their importance is even larger than elsewhere because atmospheric absorption is enhanced by the high albedo of snow and ice surfaces. In addition, the albedo of snow and ice can be reduced by BC deposition [*Clarke and Noone*, 1985; *Warren and Wiscombe*, 1981; *Hansen and Nazarenko*, 2004]. BC is a component of the so-called Arctic Haze [*Sharma et al.*, 2004], a widespread pollution phenomenon in winter and early spring that is caused mainly by long-range transport of anthropogenic emissions from Eurasia [*Barrie*, 1986]. In summer, BC concentrations (and pollution levels generally) in the Arctic are much lower [*Sharma et al.*, 2004], which is the result of slower transport from the middle latitudes [*Stohl*, 2006] and more efficient removal mechanisms than during winter [*Shaw*, 1995]. Still, the Arctic BC budget in summer is important because of the availability of shortwave radiation, the high albedo, and the large prevalence of strongly reflective low-level stratus cloud decks. Furthermore, the BC deposition load itself is relatively less reduced from winter to summer because more efficient deposition is an important reason why the BC concentrations in the air are lower in summer. Despite this large significance of light absorbing particles in summer, Arctic air pollution research has been focussed almost exclusively on the winter/spring Arctic Haze season.

[3] Our understanding of BC in the Arctic is incomplete because of the limited presence of measurement sites, conflicting ideas about sources, and varying trends in concentrations. *Sharma et al.* [2004] reported a decrease of the BC concentrations in the Canadian Arctic between 1989 and 2002, largely attributed to decreasing emissions from the former USSR. However, they also noted that BC levels stabilized in the later part of the time series. *Koch and Hansen* [2005] found that anthropogenic emissions from south Asia (which now has the worldwide largest BC emissions; *Bond et al.* [2004]) is the dominant source around the year, whereas *Stohl* [2006] suggests Europe to be the most important BC source for the Arctic in winter and argues for a possible dominance of emissions from boreal forest fires in summer in years of strong burning. Both studies, however, reported results from model simulations that are not well constrained by observations. A large uncertainty in the modeling of BC is its atmospheric lifetime, with global aerosol model studies suggesting a range of values (7.3 days, [*Koch and Hansen*, 2005]; 6 ± 2 days, [*Park et al.*, 2005]; 3–4 days [*Liu et al.*, 2005]). Recently, *Stohl et al.* [2006] showed that the most severe air pollution episode ever observed in the European Arctic and with strongly elevated BC concentrations was caused by agricultural fires in Eastern Europe.

[4] Boreal forest fires have long been recognized as an important source of aerosols for the atmosphere. For instance, observations of so-called blue moons were made both over North America and Europe after severe forest fires burning in Canada in 1950 [*Van de Hulst*, 1957; *Porch*, 1989]. More recent is the discovery that the fires also influence the atmospheric composition (e.g., CO concentrations) on a hemispheric scale [*Wotawa et al.*, 2001]. Aerosol plumes originating from these fires have been observed over downwind continents [*Van de Hulst*, 1957; *Forster et al.*, 2001] and can indeed circle the entire northern hemisphere [*Damoah et al.*, 2004]. Absorption and scattering of light in the atmosphere by smoke from boreal forest fires can cool the surface during daytime [*Robock*, 1991]. Boreal forest fires emit large quantities of BC, on average about 10% of the annual anthropogenic BC emissions in the northern hemisphere [*Lavoué et al.*, 2000; *Bond et al.*, 2004]. These emissions occur at high latitudes, are concentrated in a few summer months and have a large interannual variability. There is also a positive trend in the amount of areas burned over recent decades [*Lavoué et al.*, 2000; *Kasischke et al.*, 2005], likely because of a warming and drying in the boreal region, and this trend is predicted to continue in the future [*Flannigan et al.*, 2000].

[5] Studies of the impact of boreal forest fires on Arctic BC levels are sparse. An aircraft campaign frequently encountered aerosol plumes from Alaskan and maybe also Siberian forest fires over the Alaskan Arctic [*Shipham et al.*, 1992]. A study using satellite measurements reported that the top-of-the-atmosphere reflectivity over the snow/ice of Greenland can be reduced by as much as 60% during the passage of forest fire plumes from Canada [*Hsu et al.*, 1999]. A PhD thesis suggests a link between BC observations in Greenland and at other Arctic sites, and boreal forest fires [*Lavoué*, 2000]. There are also first speculations that deposition of BC from boreal forest fires could enhance the melting of Arctic glaciers and sea ice [*Kim et al.*, 2005], despite the fact that they occur chiefly from May to October [*Lavoué et al.*, 2000] when Arctic snow/ice cover extent is smaller than in winter. Yet, to date no study could clearly relate Arctic BC observations to forest fire activity.

[6] On average, BC emissions from temperate and boreal forest fires in Asia are more than a factor of three larger than those in North America [*Lavoué et al.*, 2000] and also have a larger potential of being transported into the Arctic [*Stohl*, 2006]. However, the impact of North American fires can be studied more easily. While fire detections from satellites are available for both regions and can be used for fire localization, in North America there are also reliable ground-based area-burnt data available, even on a daily basis. Furthermore, measurements of aerosol light absorption are performed at stations in the North American Arctic but not in northeastern Russia where the Asian fires would dominate.

[7] The summer of 2004 set a new record, 2.7 million hectare, for the annual area burnt in Alaska. This is more than ten times as much as the long-term annual average of about 0.2 million hectare [*French et al.*, 2003]. Another 3.1 million hectare burned in Canada, 50% above the long-term average [*Stocks et al.*, 2003]. Intense plumes from these fires were observed by research aircraft over large parts of North America [*de Gouw et al.*, 2006], the North Atlantic, and Europe (A. Petzold et al., unpublished manuscript, 2006). Therefore we have chosen the North American fire season of 2004 for the case study presented in this paper. We will use a Lagrangian particle dispersion model and examine measurements of particle light absorption at several sites across the Arctic to show that transport of smoke from the fires caused strong enhancements in aerosol light absorption at all stations. We will also show that transmission of shortwave radiation in the Arctic atmosphere was

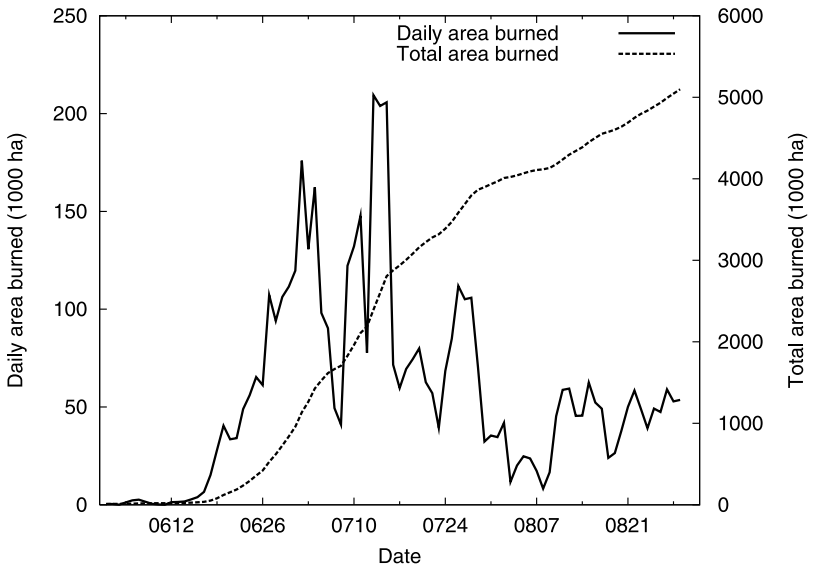

Figure 1. Daily areas burned (1000 ha) in Alaska and Canada (solid line), and total areas burned accumulated over the fire season (dashed line), from June through August 2004.

significantly reduced, and demonstrate a possible effect on the albedo of the snow in Greenland.

2. Methods

2.1. Emission Data

[8] For the transport model simulations (see below), a passive carbon monoxide (CO) tracer was used, as in previous studies [*Forster et al.*, 2001; *Spichtinger et al.*, 2001; *Damoah et al.*, 2004]. CO, similar to BC, is emitted from both biomass burning and anthropogenic combustion sources and because of its relatively long lifetime (1–2 months in summer), it is a good tracer for air masses influenced by these emission sources. A daily inventory of forest fire emissions in North America for the period 2 June until 29 August was created. Daily burned areas per province in Canada and fire province in the United States were taken from a webpage at the Center for International Disaster Information (http://www.cidi.org/wildfire) and were smoothed by calculating a 3-day running mean to reduce occasional day-to-day inconsistencies. The resulting time series for Alaska and Canada combined is shown in Figure 1. Fires started in the middle of June and continued burning into fall but daily areas burned were largest from about 26 June to 15 July. As a second source of information, MODIS fire detections (http://map.ngdc.noaa.gov/website/firedetects/viewer.htm) were counted daily on a $1^\circ \times 1^\circ$ grid, and for every 3-day period the maximum daily number of detections in a grid cell was taken in order to compensate for low detection efficiencies on cloudy days. Then, the daily areas burned in Alaska and the Canadian provinces were distributed to the grid cells in these areas, weighted by the number of fire detections. The rest of the United States was also accounted for but is not important here. Sometimes, fires were detected when no area burned was reported in a province or vice versa. This unaccounted area (about 10%) was distributed equally weighted to all fires detected during the entire period. Finally, a constant emission factor of 4500 kg CO/hectare burned was used to obtain a daily CO emission inventory on the $1^\circ \times 1^\circ$ grid. This emission factor was used previously [*Forster et al.*, 2001] and is consistent with an inversion study for the 2004 fires [*Pfister et al.*, 2005].

[9] Smoke column heights depend on fire intensity and meteorological conditions [*Lavoué et al.*, 2000], and the ideal injection height in a model also depends on model properties (e.g., resolution, convection parameterization, etc.). Here, the fire emissions were injected into the lowest 3000 m of the model atmosphere, as *Damoah et al.* [2006] found that the convection scheme in our model can be sufficiently effective to transport these emissions even into the stratosphere. Results obtained using lower injection heights were very similar because of efficient mixing in the boundary layer. Results with a higher injection height deviated more and were in less good agreement with the surface measurements but sometimes gave a better fit to aircraft observations [*de Gouw et al.*, 2006].

[10] Anthropogenic CO emission information was also used. North American emissions were based on the point, onroad, nonroad and area sources from the U.S. EPA National Emissions Inventory, base year 1999, with spatial partitioning of area sources at 4 km resolution, Mexican emissions north of 24°N and Canadian sources south of 52°N [*Frost et al.*, 2006]. Emissions elsewhere were taken from the EDGAR 3.2 Fast Track 2000 data set [*Olivier and Berdowski*, 2001]. Anthropogenic emissions were put into the lowest 100 m of the model atmosphere.

2.2. Transport Model

[11] We establish source-receptor relationships between the forest fire emissions and aerosol light absorption measurements using the Lagrangian particle dispersion model FLEXPART [*Stohl et al.*, 1998; *Stohl and Thomson*, 1999; *Stohl et al.*, 2005] (see also http://zardoz.nilu.no/~andreas/flextra+flexpart.html). FLEXPART was originally developed to simulate the dispersion of dangerous substances

from point sources and was validated for such applications with data from continental-scale tracer experiments [*Stohl et al.*, 1998]. It was used previously to study intercontinental pollution transport from forest fires [*Forster et al.*, 2001; *Spichtinger et al.*, 2001; *Damoah et al.*, 2004]. FLEXPART is a pure transport model and no removal processes were considered here. The model can therefore only be used to qualitatively relate interesting measurement episodes either to fires or to anthropogenic influence. It can neither be utilized for a quantitative comparison with aerosol data, nor to extrapolate the measurements in space and time.

[12] FLEXPART was driven with operational analyses from the European Centre for Medium-Range Weather Forecasts [*European Center for Medium-Range Forecasts*, 2002] with $1^\circ \times 1^\circ$ resolution (derived from T319 spectral truncation) and 60 model levels. There are approximately 14 model levels below 1500 m and 23 below 5000 m. In addition to the analyses at 0000, 0600, 1200 and 1800 UTC, 3-hour forecasts at intermediate times (0300, 0900, 1500, 2100 UTC) were used.

[13] FLEXPART calculates trajectories of so-called tracer particles using the mean winds interpolated from the ECMWF analyses plus random motions representing turbulence. For moist convective transport, FLEXPART uses the scheme of *Emanuel and Živković-Rothman* [1999], as described and tested by *Forster et al.* [2006]. In order to maintain high accuracy of transport near the poles, FLEXPART advects particles on a polar stereographic projection poleward of 75° but using the ECMWF data on the latitude-longitude grid to avoid unnecessary interpolation. A special feature of FLEXPART is the possibility to run it backward in time [*Stohl et al.*, 2003; *Seibert and Frank*, 2004].

[14] For this study, FLEXPART was run both forward from the fire emissions and backward in time from measurement stations. The purpose of the single forward simulation is to identify the areas most affected by fire pollution plumes and to understand the transport in relation to synoptic conditions. In total about 30 million tracer particles were released from the fire inventory grid cells, with particles carrying an equal fraction of the total mass of CO emitted. Particles were carried for 30 days, after which they were removed from the simulation. For the purpose of identifying the sources of measured air pollution, backward simulations are more accurate than forward ones since particles can be released exactly at the measurement point. Backward simulations for the Arctic measurement sites were made for every 3-hour time interval during July and August 2004. For every simulation, 40000 particles were released and followed backward in time for 20 days (for Barrow, Alert and Summit) or 30 days (for Zeppelin) to calculate a so-called potential emission sensitivity (PES) function, as described by *Seibert and Frank* [2004] and *Stohl et al.* [2003]. The word "potential" here indicates that this sensitivity is based on transport alone, ignoring removal processes that otherwise would reduce the sensitivity. The value of the PES function (in units of s kg^{-1}) in a particular grid cell is proportional to the particles' residence time in that cell. It is a measure for the simulated mixing ratio at the receptor that a source of unit strength (1 kg s^{-1}) in the respective grid cell would produce. Of special interest is the PES distribution at altitudes where emissions are likely to occur. For consistency with the forward simulations, we report PES values for a so-called footprint layer 0–3000 m above ground. Folding (i.e., multiplying) the PES footprint with the distribution of actual emission flux densities (in units of kg m^{-2} s^{-1}) from the inventory yields a so-called potential source contribution (PSC) map, that is the geographical distribution of sources contributing to the simulated mixing ratio at the receptor. Spatial integration of the PSC map finally gives the simulated mass mixing ratio at the receptor. Time series of these mixing ratios, obtained from series of backward simulations, will be presented both for fire emissions and for anthropogenic emissions. Since the backward model output is available with a daily resolution, the timing of the contributing emissions is also known.

[15] The fire emission inventory and FLEXPART backward simulations were used previously by *de Gouw et al.* [2006] and *Warneke et al.* [2006] who found relatively good agreement with aircraft measurements of CO and biomass burning tracers such as acetonitrile taken at the North American east coast. FLEXPART forward simulations were also made by *Damoah et al.* [2006] to study a pyroconvection event in June 2004 that transported fire emissions into the lower stratosphere. The simulations reported here were made with the latest FLEXPART version (6.2+) but are in close agreement with these previous studies.

2.3. Observations

[16] We report measurements from four sites located in different parts of the Arctic (Figure 2): Barrow, Alaska (156.6°W, 71.3°N, 11 m asl), Alert, Canada (62.3°W, 82.5°N, 210 m asl), Summit, Greenland (38.4°W, 72.6°N, 3208 m asl), and Zeppelin/Ny Ålesund, Spitsbergen, Norway (11.9°E, 78.9°N, 478 m asl and 50 m asl). We present measurements of light absorption from all these stations, aerosol optical depth (AOD) measurements from Barrow, Summit and Ny Ålesund, and albedo data from Summit. Despite the fact that the aerosols from the fires are also strong scatterers of light and the AOD is strongly influenced by aerosol light scattering, we concentrate on the aerosol light absorption for the surface measurements. This has several reasons: Firstly, BC (which causes most of the light absorption), is emitted directly by combustion processes and has no secondary sources, whereas light-scattering aerosols can also be produced by secondary formation processes. Secondly, data on light scattering are not available from all sites used in this study. Thirdly, light scattering and absorption were highly correlated at Barrow during the major episodes discussed here. Fourthly, only deposition of light absorbing aerosols has a substantial impact on the albedo of snow and ice.

[17] Information on light absorbing particles is gathered at Barrow, Alert and Zeppelin with particle soot absorption

Figure 2. Results of the FLEXPART forward simulation, averaged over the months of July and August 2004: (top) Total column and (bottom) mixing ratio in the lowest model layer of the forest fire CO tracer. Small black dots show all MODIS fire detections in July and August. Large black dots are drawn at the position of measurement sites.

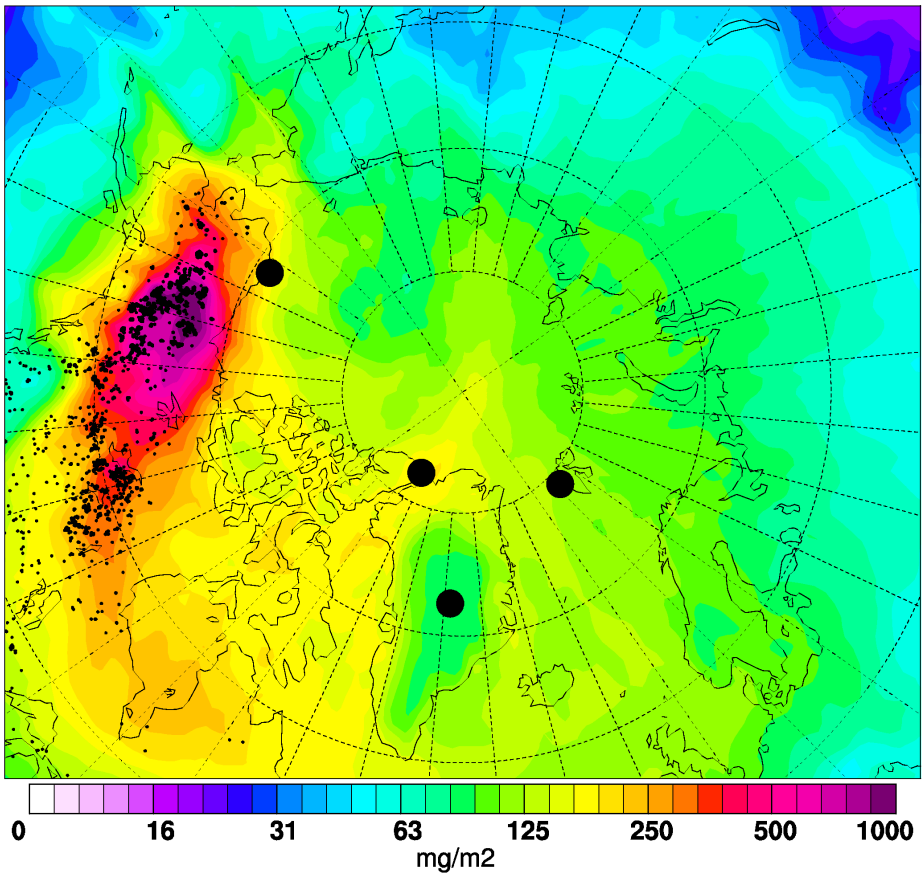

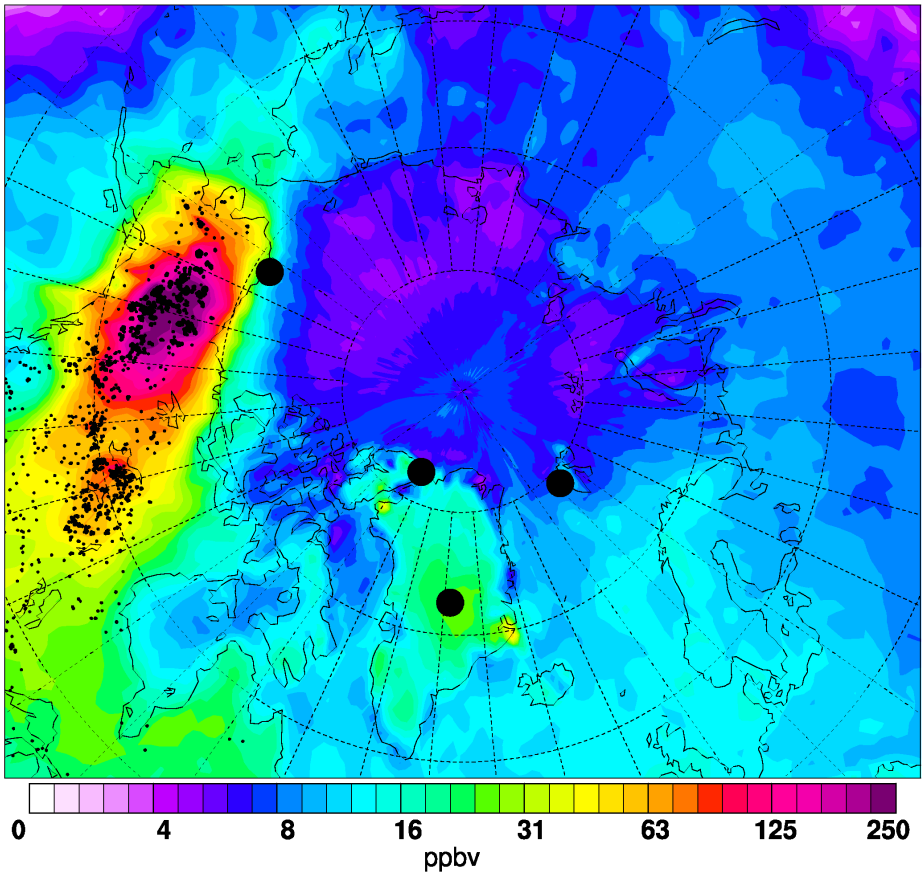

Figure 2

photometers (PSAPs) and at Summit with an aethalometer. Output from the PSAPs is given as the particle light absorption coefficient σ_{ap}, whereas aethalometer output is reported directly as BC concentrations. Conversion of σ_{ap} to BC concentrations is not straightforward. It requires the assumptions that all the light absorption measured is from BC, and that all BC has the same light absorption efficiency. Therefore we report all PSAP data directly as σ_{ap} values which can be converted approximately to BC mass concentration using a value of about 10 m^2g^{-1}, typical of aged BC aerosol [*Bond and Bergstrom*, 2005]. Since the conversion to BC in the aethalometer is done internally but relies on the same assumptions, we will refer to these data as equivalent BC (EBC) concentrations.

[18] PSAP measurements at Barrow and Alert are made as part of the standard NOAA/ESRL/GMD aerosol optical measurements system design [*Delene and Ogren*, 2002]. Briefly, a low RH (RH < 40%) sample flow passes through a 10 μm aerodynamic impactor upstream of the aerosol instrumentation. Most of this flow is sent to an integrating nephelometer to measure light-scattering by the aerosol, while a small portion ($\approx$1–2 lpm) is sampled by the PSAP (Radiance Research, Seattle, WA USA). This instrument produces a semicontinuous measurement of absorption by monitoring the change in transmittance across a filter using a 565 nm green light source. The light is split and illuminates two filter substrates. Two detectors are used, one to measure the change in optical transmission through the first filter caused by particle deposition and the other to measure variations in light source intensity through the second, particle-free filter. The change in transmitted light is related to the optical absorption coefficient using Beer's law. The absorption data are reported at a wavelength of 550 nm following corrections for sample spot size and scattering interference using the nephelometer-measured light scattering and the *Bond et al.* [1999] algorithm. PSAP measurements have been made at Barrow since October, 1997 and at Alert by Environment Canada in collaboration with NOAA since April 2004.

[19] The aerosol measurements at Barrow are normally flagged as contaminated if either the wind direction is from the contaminated sector (between 110° and 360°) encompassing the town of Barrow and some other potential sources, or particle number concentrations are above 8000 cm^{-3}. The smoke events discussed here would have been marked as contaminated because the wind came from the contaminated sector. It was decided to ignore the wind-screening for the purpose of this study because the measured aerosol properties were one to two orders of magnitude higher than typically measured when the air was from the contaminated sector. Furthermore, there is auxiliary evidence that the episodes reported here were due to large-scale smoke, not local contamination (see below). No screening for local pollution was performed for the Alert data but winds at Alert during the major episode discussed below were not from the contaminated sector. Some of the smaller enhancements could be due to sources in the nearby military base camp, and data from 6 to 21 August cannot be used because of military truck and aircraft operations and the annual import of fuel for the camp.

[20] σ_{ap} measurements at Zeppelin are performed using a custom built PSAP. The measurement principle is the same as described above, but here the light (530 nm) illuminates two 3 mm diameter spots on a single filter substrate rather than utilizing two separate filters. In order to maximize the time one can use a filter substrate and to have a similar rate of change in the light transmission despite changing ambient concentrations, a flow control system that regulates the sample mass flow according to the concentration levels is used. Scattering corrections are not used for these data. As there are no significant pollution sources in the vicinity of the station, no screening for local contamination was performed.

[21] At Summit, data are collected with a 1 channel aethalometer from Magee Scientific Company. The aethalometer is a self contained instrument that uses a similar measurement principle as the PSAPs. The conversion of light absorption to EBC is done internally using manufacturer supplied procedures. To exclude possible contamination from camp pollution, local wind information was used to exclude periods with winds from the northerly sector (247°–112° for wind speeds less than 5 m s^{-1}, 300°–50° otherwise).

[22] The responses of both the PSAPs and the aethalometer depend on the loading of particles on the filter and on the amount of light that the particles scatter [*Bond et al.*, 1999; *Weingartner et al.*, 2003; *Arnott et al.*, 2005]. The Barrow and Alert PSAP data were corrected for these dependencies according to the procedure described by *Bond et al.* [1999]. For dry mixtures of kerosene soot and ammonium sulfate in the laboratory, *Sheridan et al.* [2005] showed that the *Bond et al.* [1999] corrections yield results that agree within about 10% of the average of two independent reference methods. At the Zeppelin station, nephelometer data would in principle also be available to correct the PSAP data, like for Barrow and Alert. However, for the purpose of this study, a constant enhancement factor of 2 was used instead, which could lead to a tendency to overestimate the σ_{ap} by typically 50%. For the aethalometer, *Arnott et al.* [2005] reported that "simultaneous aerosol light scattering measurements are required for accurate interpretation of aethalometer data for high aerosol single-scattering albedos. Instantaneous errors of up to ±50% are possible for uncorrected data, depending on filter loading."

[23] In March 2000 NOAA Global Monitoring Division began making continuous 1-min resolved measurements of spectral irradiance to derive estimates of AOD at Barrow. In 2004 a 4-channel Sun-photometer was in operation. During sunlit hours of the day AOD at 412, 500, 675, and 865 nm were computed and filtered to eliminate cloud effects. Further details of the program are given by *Stone* [2002].

[24] AOD measurements at 368, 412, 500 and 862 nm have also been carried out at Summit and in Ny-Alesund, about 2 km from Zeppelin at 50 m asl, since May 2002 [*Hermansen et al.*, 2005] with precision-filter-radiometers (PFR) as part of the Global Atmsopheric Watch (GAW) radiometer trial network [*Wehrli*, 2005]. Instruments are calibrated every year at the World Radiation Center in Davos, and the data have undergone cloud clearing and quality control following the GAW network routines. For Ny Ålesund, additional measurements with the Sun-photometer SP1A [*Herber et al.*, 2002] have been performed since 1991 at the German-French research base. The SP1A uses the same wavelength as the PFR and provides compa-

rable AOD data and, thus, the two data sets have been merged to provide the best data coverage. Data points sandwiched in between others flagged as cloud contaminated have been removed.

[25] CO measurements at Zeppelin are used to identify the period influenced by the forest fire emissions at this site. Measurements are made using a RGA3 analyzer (Trace Analytical) fitted with a mercuric oxide reduction gas detector. Five ambient air measurements and one field standard are performed within a time period of 2 hours. The field standards are referenced against a Scott-Marine Certificated standard and a calibration scale developed at CSIRO (Commonwealth Scientific and Industrial Research Organization). Detailed descriptions of the CSIRO scale, including the methods used, and the evaluation of its long-term stability are given by *Langenfelds et al.* [1999] and *Francey et al.* [1996].

[26] All σ_{ap} and EBC values are averaged here to 3-hourly mean values, for comparison with the model results. CO data are kept at the original 2-hour resolution. AOD measurements are done at irregular intervals and are reported as instantaneous values for Barrow and Ny Ålesund but were averaged to 1-hour-mean values for Summit.

[27] At Zeppelin, analysis of the aerosols' content of levoglucosan, a well-known tracer of particulate emissions from biomass burning, was performed using high-performance liquid chromatography combined with time-of-flight high-resolution mass spectrometry (HPLC/HRMS-TOF) and according to the methodology described by *Dye and Yttri* [2005]. The methodology holds the combined merits of short preparation, high sensitivity and complete separation of levoglucosan from its isomeric compounds, as evaluated by *Scholnik and Rudich* [2006]. The aerosols were collected on $8'' \times 10''$ cellulose filters (Whatman 41) according to a 2 + 2 + 3 days weekly sampling scheme, using a high volume sampler with a 2.5 μm cut off. The filters were made available from the AMAP (Arctic Monitoring and Assessment Program) heavy metal monitoring in the Arctic.

[28] To determine possible effects of the deposition of light absorbing aerosols on the albedo of a snow surface, we use radiation measurements at Summit, Greenland. Shortwave radiative fluxes (direct solar, diffuse, global, shortwave reflected) are monitored by ETH Zurich at 2 m above ground, closely following the high quality standards of the Baseline Surface Radiation Network (BSRN) [*McArthur*, 1998]. Direct solar radiation is measured with a pyrheliometer (Kipp & Zonen CH1), diffuse, global and shortwave reflected radiation with Kipp & Zonen CM21 pyranometers. The pyranometers are ventilated with an air-stream heated slightly above ambient temperature to keep the instrument domes free of rime at all times.

3. Results

[29] Figure 2 shows results from the FLEXPART forward tracer simulation, averaged over the months of July and August 2004, which indicate the major areas affected by the forest fire plumes over 30 days of transport. Both in the CO tracer total atmospheric column plot (Figure 2, top) and in the surface mixing ratio plot (Figure 2, bottom), strong maxima are seen in the burning region. Away from the source region, tracer distributions for the entire column and at the surface are very different. When considering the total atmospheric column, the central Arctic is impacted strongly compared to the middle latitudes. At the surface, in contrast, the central Arctic is relatively less affected compared to the middle latitudes, suggesting lifting of the forest fire plumes upon transport into the Arctic. This is consistent with the fact that surfaces of constant potential temperature form closed domes over the Arctic, with minimum values in the Arctic boundary layer [*Klonecki et al.*, 2003; *Stohl*, 2006]. The polar dome concept suggests that air masses must rise when they enter the Arctic. In the process of the lifting, washout would remove a large fraction of the aerosols initially present in the plumes and deposit them in the Arctic. Even though the Arctic lower troposphere is less affected, our measurement stations are ideally located: Barrow is relatively close to the source region (about 1000 km away); Summit, at an altitude of 3200 m, is influenced more strongly than areas at sea level (Figure 2, bottom); Alert and Zeppelin are located in areas affected much less by the fire plumes. As will be shown, these differences are reflected in the measurement data.

[30] Figure 3 shows a time series of 3-hour average σ_{ap} values at Barrow for July 2004 (black line) and the corresponding time series of FLEXPART CO tracers from forest fires (colored bars) and anthropogenic emissions (red line), as obtained by 20-day backward simulations initialized every 3 hours at Barrow. The forest fire CO tracer is colored according to its "age," i.e., time since emission, whereas for the anthropogenic CO tracer only the 20-day total is shown. The simulated CO tracer mixing ratios from forest fires are generally much larger than those from anthropogenic sources. Many of the observed spikes in σ_{ap} (including the five highest values) occur almost exactly at the same time as simulated maxima in forest fire CO. There are also a few smaller simulated spikes that do not show up in the measurement data. A possible explanation for this is that the light absorbing particles were removed from these air masses but more likely it is the result of the coarse space and time resolution of the emission inventory, which causes the model to generate additional episodes. Anthropogenic emissions explain little of the σ_{ap} variation but the lowest values (e.g., on 6–7 July) were measured when both anthropogenic and forest fire CO tracer mixing ratios are low. The frequency at which forest fire plumes influenced the station is remarkable. Several other episodes of smaller magnitude (not shown) occurred in August.

[31] According to lidar measurements at Barrow (not shown), there was even more smoke aloft. AOD measurements show greatly enhanced values above the normal background throughout much of July (Figure 4, symbols) and FLEXPART also suggests forest fire plumes passing over Barrow almost continuously (Figure 4, solid line). The episode on 2–4 July is particularly noteworthy as this plume continued travelling deep into the Arctic and shall be discussed in more detail in the following. Beginning around 2100 UTC on 2 July, a time when micropulse lidar backscatter returns indicate aerosols aloft between about 250 and 3500 m altitude (not shown), AOD values increased strongly. Good retrievals were made for several hours with peak visible (500 nm) values exceeding 1.2 units before the signal was lost because of low Sun angles. Beginning around 1200 UTC on 3 July and lasting for

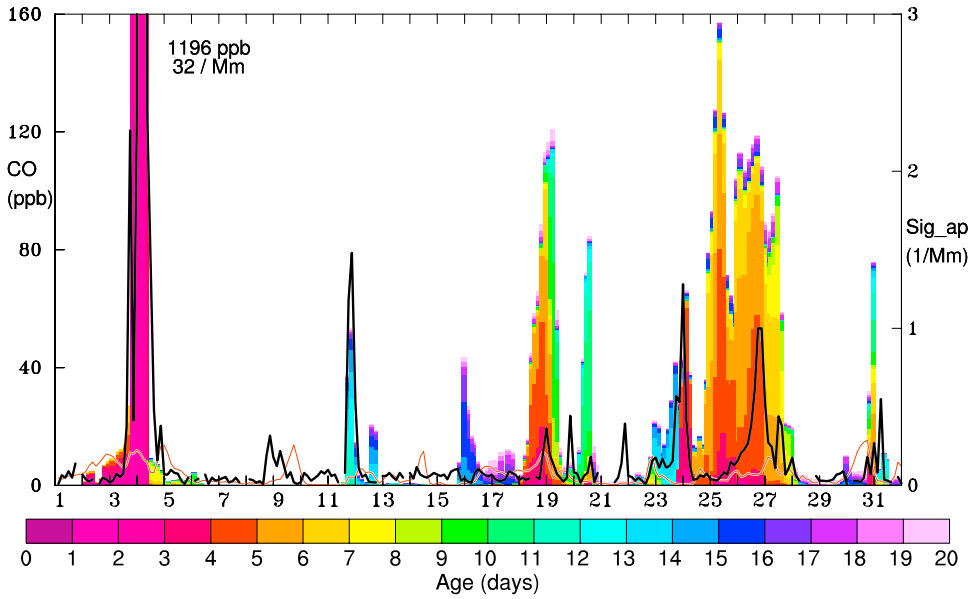

Figure 3. Comparison of the time series of 3-hour mean σ_{ap} values measured by the PSAP (black line, in Mm^{-1}) and CO tracer mixing ratios (ppb) obtained from the FLEXPART backward simulations, for Barrow for July 2004. Anthropogenic CO tracer, accumulated over all 20 days of transport, is shown by the red line, whereas North American forest fire CO tracer is shown as stacked bars whose color indicates its age, i.e., the time passed since emission at the fire locations. Numbers near the top indicate modeled and measured values outside the data range shown in the plot.

about four hours a rare thunderstorm occurred at the site; heavy rain fell during the night. By 1700 UTC the skies cleared and the smoke was again observed and even thicker. The smoke totally attenuated the shorter wavelengths of the Sun-photometer so we do not have data for this period. On the basis of measurements at 675 and 865 nm, however, AOD at 500 nm probably exceeded 3 units. By 0000 UTC on 4 July a pulse of dense smoke engulfed Barrow and was also observed at the surface (Figure 3). Because the intrusion of smoke at the surface occurred at a time when Sun elevation was low and the smoke was so thick, again no AOD data are available. All channels totally attenuated suggesting visible AOD may have exceeded 4–5 units, unprecedented in the NOAA records. It should be noted that

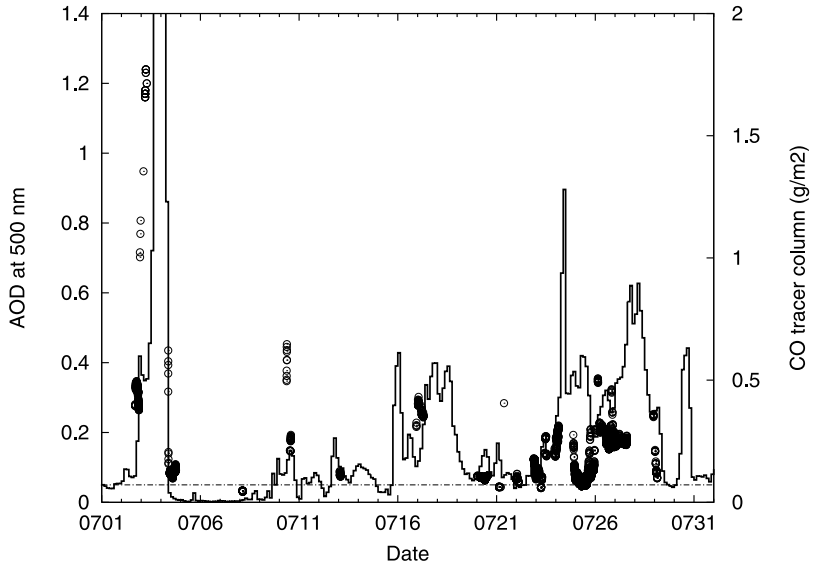

Figure 4. Comparison of AOD measurements at 500 nm at Barrow (symbols) and FLEXPART CO tracer columns above Barrow from the forward simulation (solid line), for July 2004. The horizontal dashed line indicates typical background AOD at Barrow. On 3 and 4 July, at times the sky was so opaque that AOD measurements saturated but are estimated at above 3 units and 4–5 units, respectively (not shown).

Table 1. Comparison of σ_{ap} and EBC Values During the Forest Fire Episode With Climatological Values[a]

Station	Episode Maximum	Jul–Aug 2004	Summer	March	Annual	Period
Barrow σ_{ap}	34.00	0.04	0.05	0.44	0.17	Jan 1998 to Dec 2005
Alert σ_{ap}	0.71	0.03	-	0.36	0.17	Jan 2004 to Dec 2004
Alert, aethalometer σ_{ap}	-	-	0.08	1.23	0.50	Jan 1998 to Dec 2002
Zeppelin σ_{ap}	0.63	0.05	0.05	0.47	0.11	Oct 2002 to Aug 2005
Summit EBC	828	41.5	20.2	12.8	14.5	Aug 2003 to Jan 2006

[a]Values of σ_{ap} are in Mm^{-1}, and values of EBC are in ng m^{-3}. Reported are the maximum 1-hour-mean value during the forest fire episode, the median for July and August 2004, and the median values measured during summer (June, July, August), in March, and annually, for the four Arctic stations. Periods over which long-term medians are calculated are given in the last column. For Alert, PSAP measurements are available only for the year 2004 but aethalometer data from previous years, converted to σ_{ap} using 19 m^2 g^{-1} [*Sharma et al.*, 2004], are also shown.

the large AOD values are mainly a result of light scattering by the smoke aerosols, not of light absorption; in fact, the measured single-scattering albedo of the smoke aerosol was 0.96.

[32] At the ground, the two 3-hour-mean σ_{ap} values from 0000–0600 UTC are 32 and 14 Mm^{-1}, and the corresponding model CO tracer mixing ratios are both almost 1200 ppb (Figure 3). Unfortunately, no CO monitoring data are available for Barrow for summer 2004 to check the extremely high model values. However, no other values of $\sigma_{ap} > 10$ Mm^{-1} have been observed at Barrow during the years 2000–2004, except for two other episodes in summer 2003 that might also have been caused by forest fires. Even during the Arctic Haze season, normally the most polluted time of the year, few σ_{ap} values exceed 1 Mm^{-1} and medians in March are only 0.44 Mm^{-1} (Table 1). Thus the PSAP data confirm the presence of an extraordinarily strong plume, as suggested by the model. The age of the CO tracer for this episode is 4 days, indicating fast transport from the fire region.

[33] Figure 5 shows PES and fire CO PSC maps from the backward calculations for the Barrow surface site for the period 0300–0600 UTC on 4 July. The vertically integrated PES map shows that the air mass came from the west and passed close to Barrow about a week before arrival (Figure 5, top), with most of the air passing at an altitude of about 3500 m north of Barrow, and some air coming from further south and from altitudes below 3000 m. The air travelled further east to about 130°W from where it looped around a high-pressure system. This anticyclone was located just north of the most active fires and the recirculating air mass descended into the boundary layer exactly over the region where most of the fires burned, resulting in very high PES footprint values in this critical region (Figure 5, middle). The result is very large simulated CO PSC values from many of the fires (Figure 5, bottom), whose area integration gives the extremely large total simulated CO mixing ratio of 1200 ppb for Barrow. Backward simulations for just six hours later, when the anticyclone had moved further east, show air coming to Barrow straight from the west, no longer taking up the fire emissions.

[34] Total CO tracer columns from the FLEXPART forward simulation for 30 June, 2 July, 3 July and 4 July (Figure 6) show an accumulation of fire emissions in the region south of the fires at the end of June (Figure 6, first panel) after a period of intense burning (Figure 1), advection of the plume to the west on the southern end of the anticyclone (Figure 6, second panel), northward on its western edge (Figure 6, third panel) and finally northeastward (Figure 6, fourth panel). There was convective lifting but most of the plume remained in the lower troposphere (not shown), because of the subsidence in the anticyclone.

[35] As the anticyclone retreated on 4 July, a low-pressure system moved in from the west, north of Alaska. Its cold front pushed the pollution northwestward and wiped Alaska clean but sent a big pulse of pollution to the central Arctic. A MODIS Terra satellite image for 1935 UTC on 5 July (Figure 7, right) shows a river of pollution flowing into the Canadian Arctic to almost 80°N. The plume is also seen in the corresponding map of the FLEXPART CO tracer total column for 1800–2100 UTC (Figure 7, left), which is well correlated with the aerosol features seen in the MODIS image. A vertical section through the FLEXPART model output along 120°W at the same time (Figure 8) suggests that the warm conveyor belt (WCB) [*Eckhardt et al.*, 2004] associated with the encroaching cyclone lifted the plume to altitudes of up to 6–7 km (the pollution even higher up was due to deep convection over the fires, see *Damoah et al.* [2006]). The maximum plume altitudes in the leading part of the plume further east, are lower (4 km at 100°W). The satellite image (Figure 7, right) shows that the pollution plume at this time was still in a cloud-free environment, except for its higher trailing part where WCB clouds were starting to form. Satellite images on the following days still show streams of smoke at high Arctic latitudes but less clearly than on 5 July because of increased cloudiness hampering satellite detection, and possibly because precipitation removed a large fraction of the aerosols.

[36] Parts of the plume remained relatively low and, thus, were also detected at Alert where aerosol light absorption levels were enhanced from 6 to 8 July, exactly during the period when FLEXPART backward simulations suggested the strongest influence from the fires (Figure 9). CO measurements at the site (D. Worthy, personal communication, 2006) show a moderate increase of about 20 ppb at the same time, which confirms the presence of the forest fire plume but also shows that FLEXPART overestimates its impact at Alert. PES maps (not shown) indicate that the

Figure 5. Results from the FLEXPART backward simulation initialized at Barrow at 0300–0600 UTC on 4 July 2004. Shown are (top) the column-integrated PES map with numbers labelling the plume centroid position at daily intervals, (middle) the PES map for the lowest 3 km above ground with black dots indicating MODIS fire detections for the period 29 June til 1 July, and (bottom) the forest fire CO PSC map.

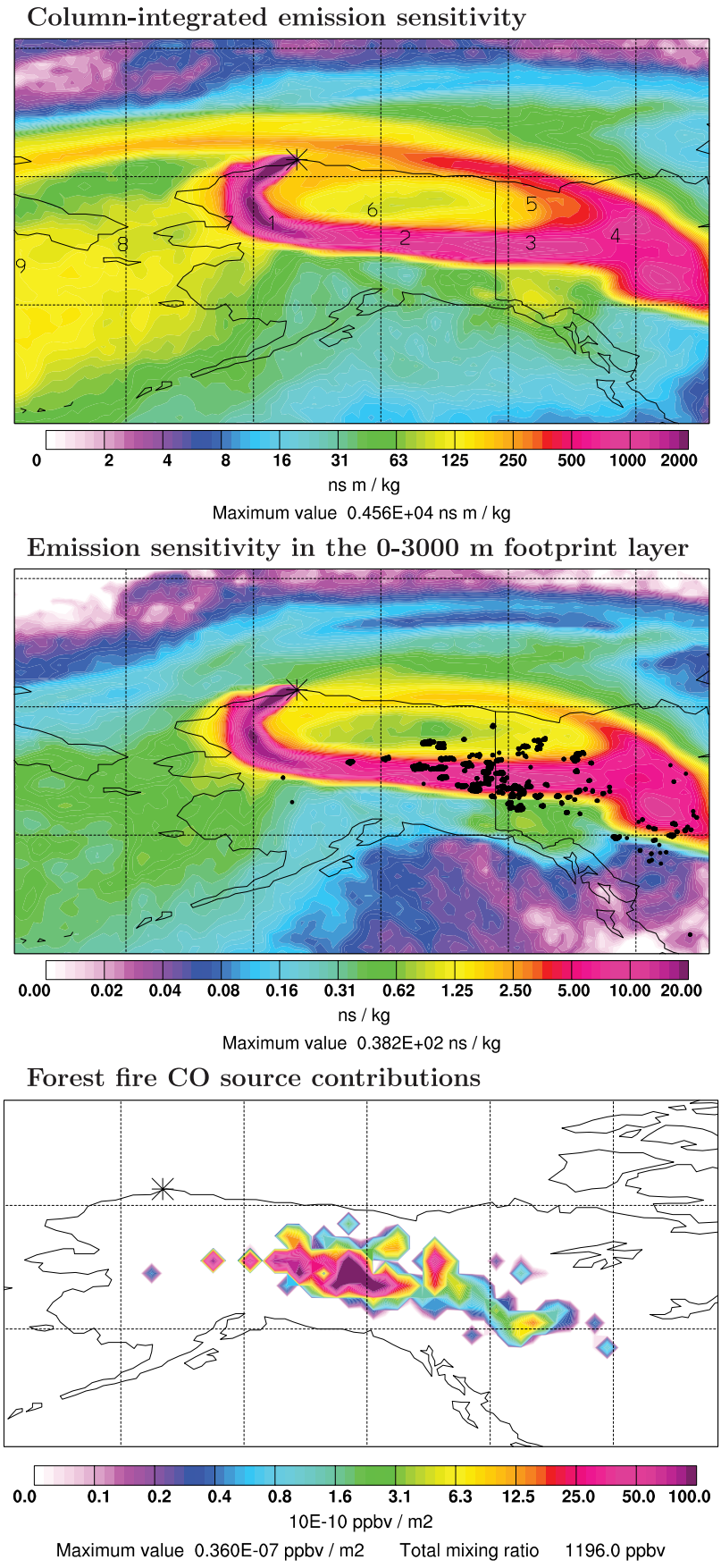
Column-integrated emission sensitivity
1
2
3
4
5
6
7
8
9
0 2 4 8 16 31 63 125 250 500 1000 2000
ns m / kg
Maximum value 0.456E+04 ns m / kg
Emission sensitivity in the 0-3000 m footprint layer
0.00 0.02 0.04 0.08 0.16 0.31 0.62 1.25 2.50 5.00 10.00 20.00
ns / kg
Maximum value 0.382E+02 ns / kg
Forest fire CO source contributions
0.0 0.1 0.2 0.4 0.8 1.6 3.1 6.3 12.5 25.0 50.0 100.0
10E-10 ppbv / m2
Maximum value 0.360E-07 ppbv / m2 Total mixing ratio 1196.0 ppbv

Figure 5

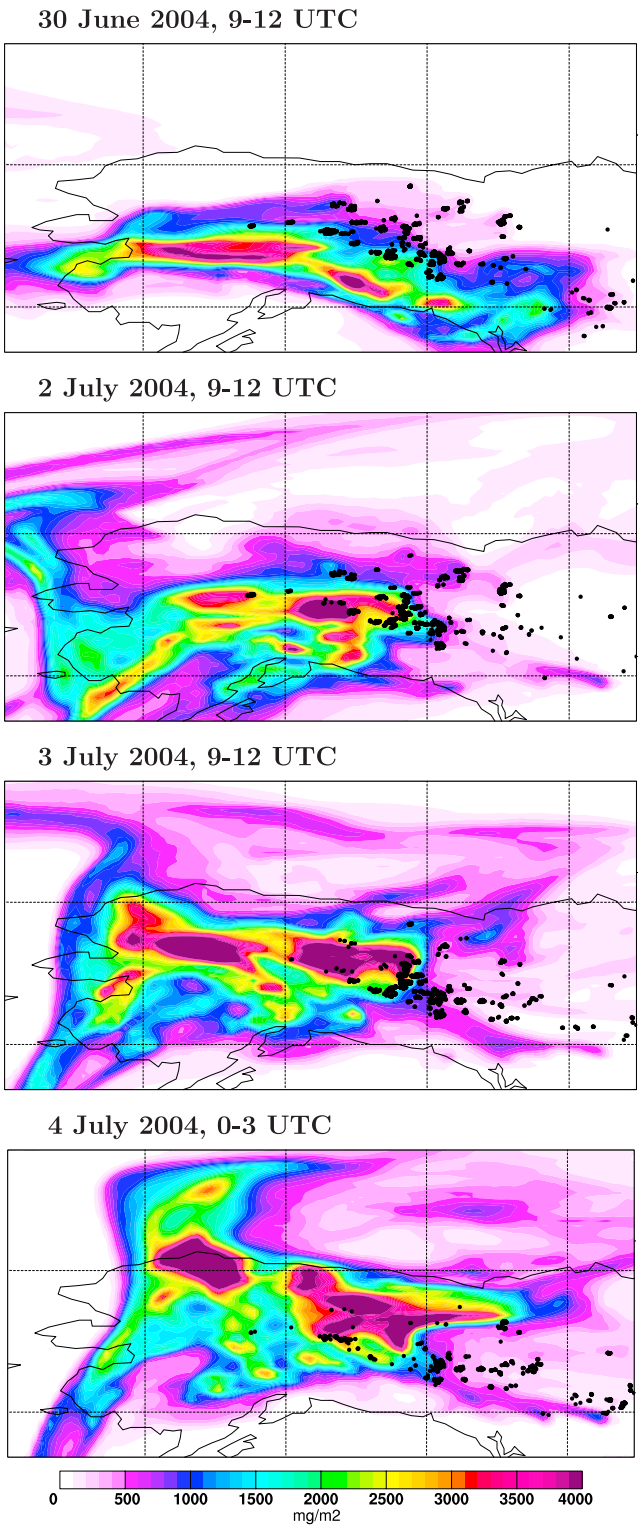

Figure 6. Total column of CO tracer from the forward simulation, shown for 30 June 2004, 0900–1200 UTC (first panel); 2 July, 0900–1200 UTC (second panel); 3 July, 0900–1200 UTC (third panel); and 4 July, 0000–0300 UTC (fourth panel). Black dots show the MODIS fire detections on the respective day.

polluted air masses originated from the same burning region and at about the same time as those observed at Barrow a few days earlier. For the rest of the month, both σ_{ap} and forest fire CO tracer maxima are not particularly high, indicating that no other strong plume affected Alert. Furthermore, the local wind direction indicates frequent transport from the nearby military base camp, making local contamination a likely reason for much of the σ_{ap} variation.

[37] According to the model results, the forest fire plume reached the north pole on 8 July. Unfortunately, satellite images do not show the smoke because of dense cloud cover, and there are no other measurements available near the pole. Furthermore, the model suggests additional transport events to the Arctic later in July and also in August. Some of them were similar to the one discussed above and caused other σ_{ap} peaks at Barrow (see Figure 3). Others were quite different and involved transport over the Atlantic Ocean. Plumes travelling south of the southern tip of Greenland were occasionally transported to the Arctic at the end of the North Atlantic stormtrack. Much of the BC in these air masses was likely scavenged before they reached the Arctic. Plumes leaving North America at higher latitudes, however, were often blocked by Greenland's topography and redirected to the north over Baffin Bay. The FLEXPART simulation shows at least two major plumes taking this route (see Figure 2, top).

[38] The almost continuous transport of smoke into the Arctic can best be seen in the AOD measurements from Summit (Figure 10). During July and August, for which FLEXPART predicts frequent transport of smoke through the column over Summit, almost every single AOD measurement there was clearly elevated over normal background values. Maximum AOD values reached about 0.4–0.5 units. Aethalometer measurements of EBC at Summit in July and August are also well above the normal background typical for the site in summer (see Table 1) and two transport events are especially clear (Figure 11). During the first period, from 16 to 20 July, a major plume impinged on the west of Greenland. Most of it was redirected deep into the Arctic, as described above, but some filaments were sheared off and reached the interior of Greenland. Because these filaments were rather small-scale features, FLEXPART suggests large variability in the CO tracer concentrations at Summit from 16 to 20 July. The aethalometer measurements also show several peaks and large variability during this period. As this air mass remained far north, anthropogenic BC contributions are negligible and, thus, the measured EBC must come from the forest fires.

[39] During the second episode from 2 to 5 August, a rather fresh forest fire plume (age less than 6 days) arrived at Summit. EBC concentrations during the episode are strongly elevated above the normal background for more than 2 days, with peaks up to 600 ng m^{-3}. Again, the model-simulated anthropogenic contributions during the passage of the fire plume are very low. Shortly later, the model also suggests the arrival of an anthropogenic plume and, thus, the additional EBC peak on 5 August might be of anthropogenic origin.

[40] The last Arctic site for which σ_{ap} measurements are available to us is Zeppelin which is located in a relatively unaffected part of the Arctic (Figure 2). Still, the model suggests that air masses moderately affected by the forest

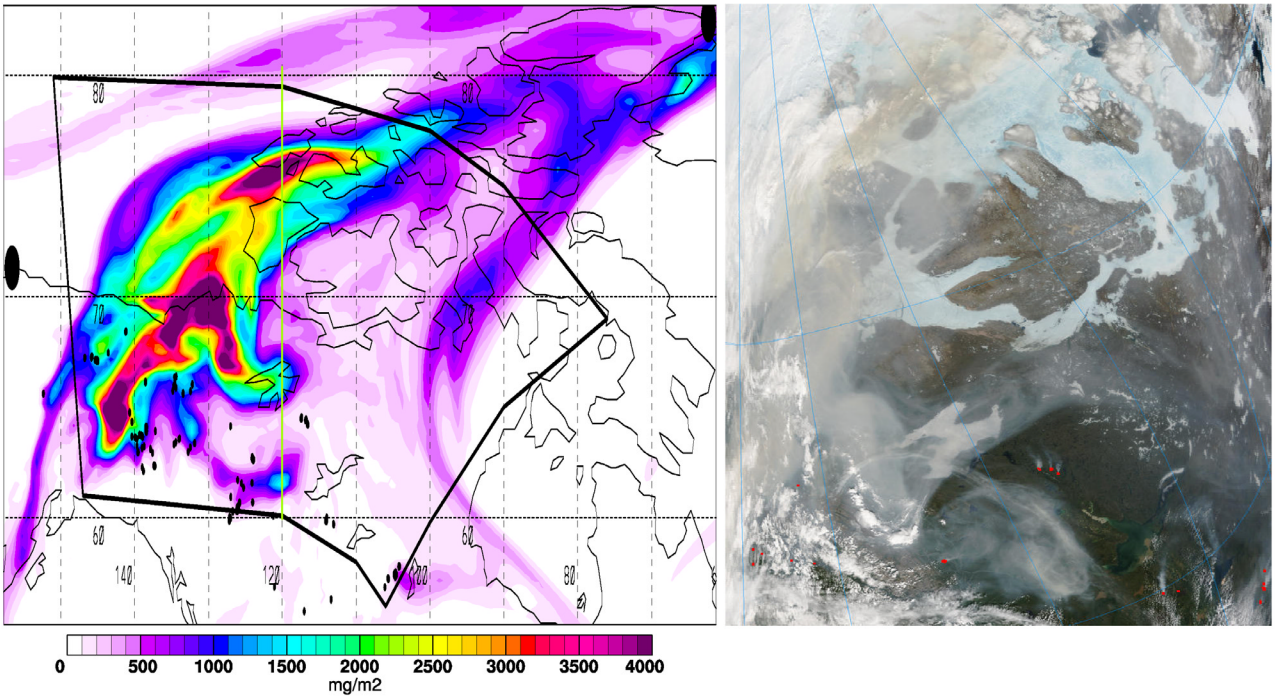

Figure 7. (left) Total columns of the FLEXPART CO tracer at 1800–2100 UTC and (right) MODIS Terra image at 1935 UTC on 5 July 2004. The approximate region shown by the MODIS image is indicated by the thick black line in the CO tracer plot, and the green line indicates the position of the vertical section shown in Figure 8. MODIS fire detections are shown as black and red dots in the left and right images, respectively. Detections are for the entire day on the left plot but only for the respective MODIS Terra image in the right plot. Large black dots in the left image indicate the locations of Barrow on the far left and Alert in the top right corner. Note the strong distortion of the MODIS image, especially at the far left and right.

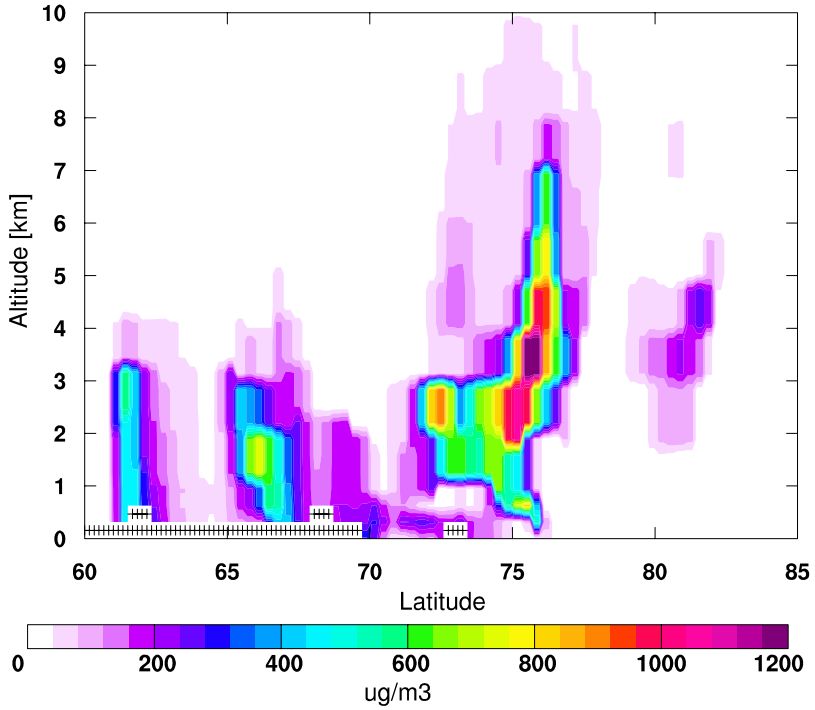

Figure 8. Vertical section from 60°N to 85°N through the FLEXPART CO tracer along 120°W at 1800–2100 UTC on 5 July 2004.

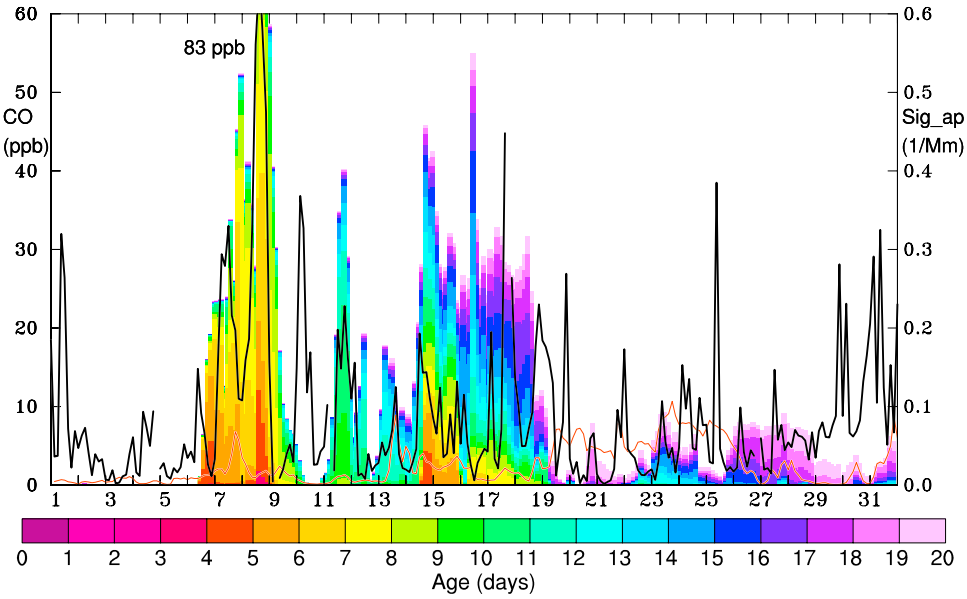

Figure 9. Same as Figure 3 but for Alert.

fires arrived at Zeppelin between about 21 July and 13 August after transport times of 3 to 4 weeks (Figure 12). After such a long time, the air masses that originally received the fire emission input are well mixed with cleaner air and FLEXPART also suggests an admixture of anthropogenic emissions (Figure 12, bottom).

[41] CO measurements at Zeppelin show a clear anomaly in their seasonal variation. Normally, CO concentrations are highest in winter and decrease to a minimum in July and August. During the year 2004, CO values reached a minimum of about 85 ppb in the middle of July but increased to about 110 ppb during the suggested period of strong fire influence (Figure 13), with peaks of 130 ppb for 2-hour mean values (Figure 12, bottom). In the middle of August, after the fire influenced period, CO values decreased again to about 95 ppb. Thus the North American forest fires left a clear anomaly in the summertime CO levels at Zeppelin, similar to what was found for the entire northern hemisphere in previous studies of strong fire years [*Wotawa et al.*, 2001; *Novelli et al.*, 2003; *Spichtinger et al.*, 2004]. At the same time, some of the higher-frequency CO variations even during the period influenced by fire emissions is also due to the transport of anthropogenic emissions. The FLEXPART anthropogenic CO tracer (red line in Figure 12, bottom) actually reproduces the timing of many of the measured CO maxima quite well. However, the generally enhanced CO levels (i.e., the seasonal anomaly of about 20 ppb or more) during the suggested passage of

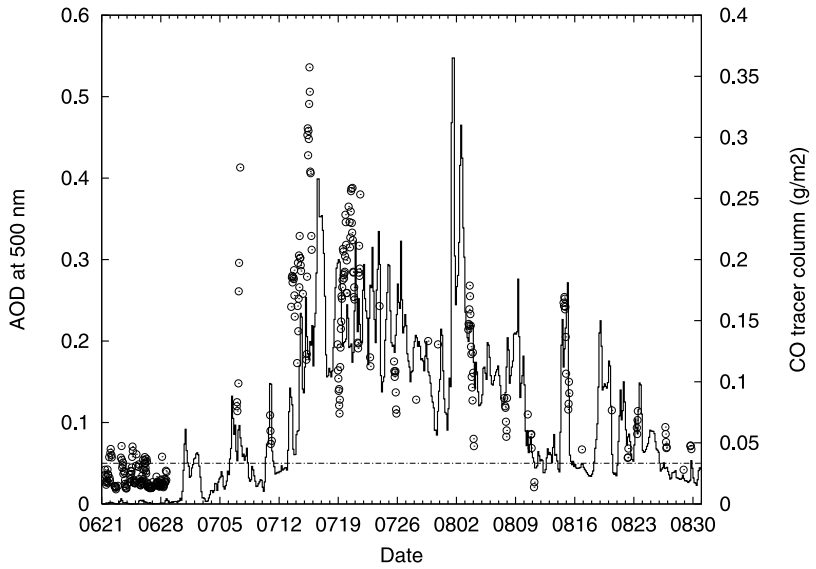

Figure 10. Comparison of AOD measurements at 500 nm at Summit (symbols) and FLEXPART CO tracer columns above Summit (solid line), for 21 June til 30 August 2004. The horizontal dashed line indicates typical background AOD at Summit.

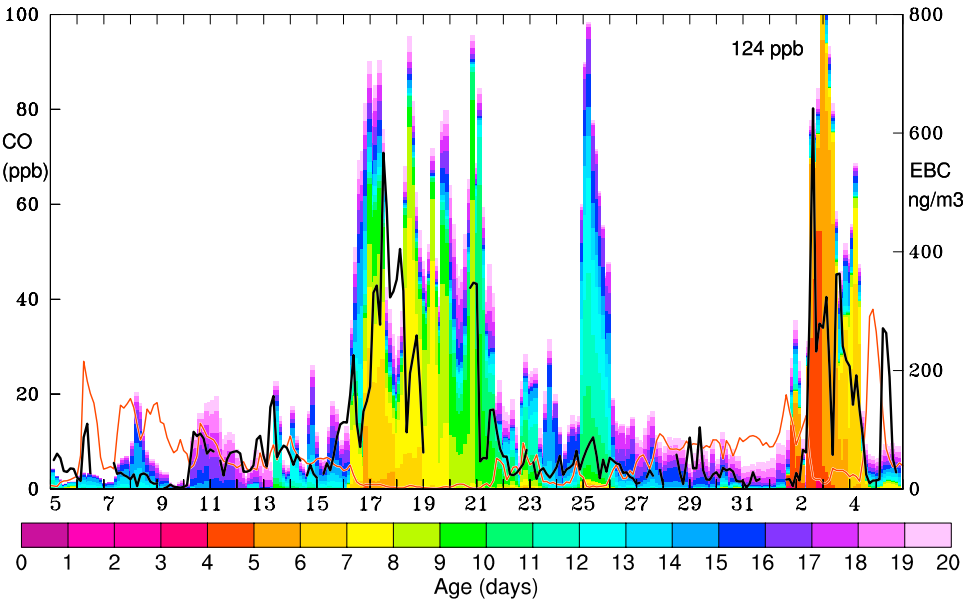

Figure 11. Same as Figure 3 but for Summit, for the period 5 July til 5 August 2004. Instead of σ_{ap}, EBC concentrations (ng m^{-3}) from the aethalometer are shown.

the fire plume cannot be explained by anthropogenic CO. This additional CO is well explained by the forest fire CO tracer values of about 20–40 ppb. Unfortunately, measurements of chlorofluorocarbons that could help separate fossil fuel combustion from biomass burning contributions are not available.

[42] Values of σ_{ap} are not particularly high during most of the period with forest fire influence (Figure 12, top).

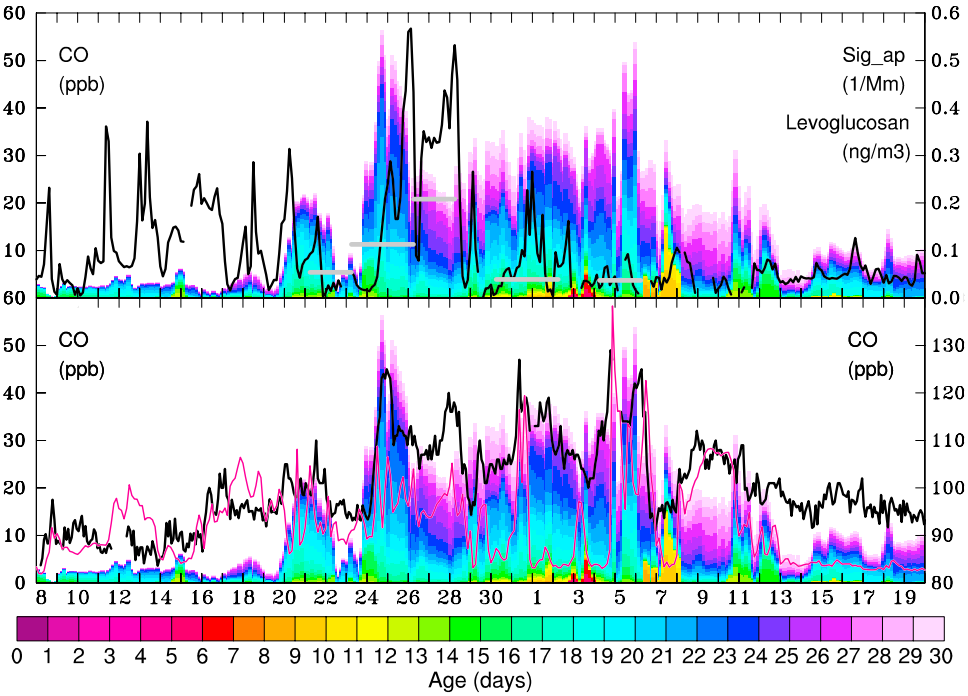

Figure 12. (top) A comparison of the time series of σ_{ap} measured by the PSAP (black line, in Mm^{-1}) and the forest fire CO tracer age spectra (colored stacked bars, ppb) obtained from 30-day FLEXPART backward simulations made every 3 hours, for Zeppelin, for the period 8 July to 19 August. Also shown in are the concentrations of levoglucosan in irregular aerosol filter samples (light grey horizontal lines). (bottom) Repeats the FLEXPART forest fire tracer results from Figure 12 (top). In addition, it shows the anthropogenic CO tracer accumulated over all 30 days of transport (red line, scale on the left axis) and CO mixing ratios measured at Zeppelin (black line, scale on the right axis).

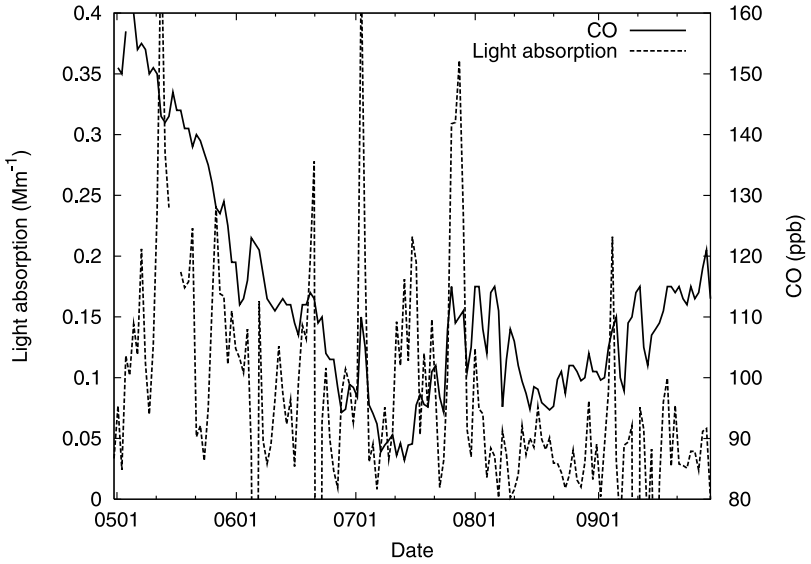

Figure 13. Time series of daily mean CO and σ_{ap} measured at Zeppelin between 1 May and 30 September 2004.

However, there is a period from 25 to 28 July with σ_{ap} values of up to 0.6 Mm^{-1}. This is when FLEXPART suggests the arrival of the strongest plume from the North American forest fires. FLEXPART shows that the fire plume is mixed with anthropogenic emissions, such that an unambiguous attribution of the strong light absorption to fire emissions is difficult. However, a remarkable feature is that the σ_{ap} values remain high during a period of 4 consecutive days, which indicates the passage of a broad aged plume from a distant source. Figure 13 shows that this case indeed stands out in summer 2004 as the only one with $\sigma_{ap} > 0.3$ Mm^{-1} for several consecutive days.

[43] Levoglucosan is the most recognized marker for tracing emissions of particulate matter from biomass burning. It is emitted in high concentrations, it is not present in the vapor phase, it is associated with fine aerosols exclusively, and it is not selectively removed from the atmosphere [*Simoneit et al.*, 1999]. These highly desired qualities enable detection of plumes from biomass burning over vast distances, even on the intercontinental scale [*Fraser and Lakshmanan*, 2000]. We analyzed a number of filter samples that were available from the AMAP monitoring program at Zeppelin. The data obtained, shown as grey horizontal lines in Figure 12 (top), positively confirm that the aerosols at Zeppelin during the period 25–28 July were indeed produced primarily by biomass burning. Daily measurements of potassium, another, albeit less specific, tracer for biomass burning, are also available from Zeppelin. All measured concentrations during the period shown in Figure 12 were below the detection limit, except for those taken on 23, 25, 27 and 28 July, and 6 and 7 August. This, again, points toward the biomass burning source of the aerosols observed from 25 to 28 July.

[44] Figure 14 shows the column-integrated PES function for the FLEXPART backward calculation started at Zeppelin at the time of the σ_{ap} maximum. The plot shows a well-defined history of the air mass only for about 3 days back when it bifurcated (back in time; forward in time two air

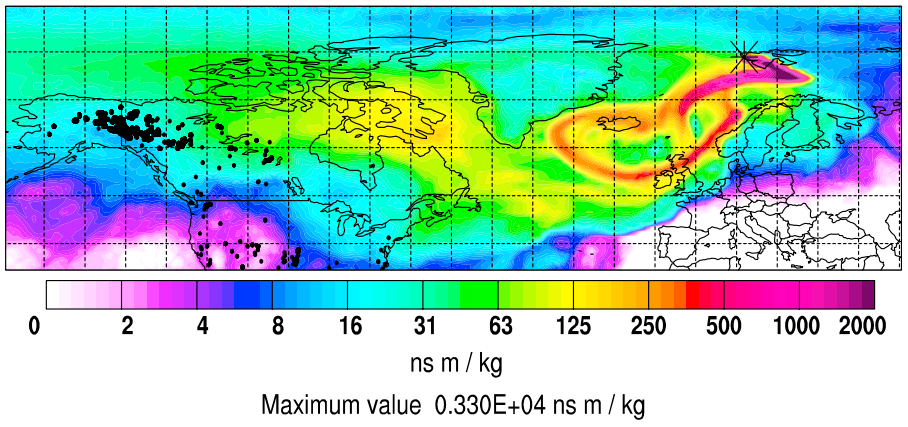

Figure 14. Column-integrated PES map for the FLEXPART backward simulation initialized at Zeppelin at 0000–0300 UTC on 26 July 2004. MODIS fire detections in North America for the period 1–10 July are shown as black dots.

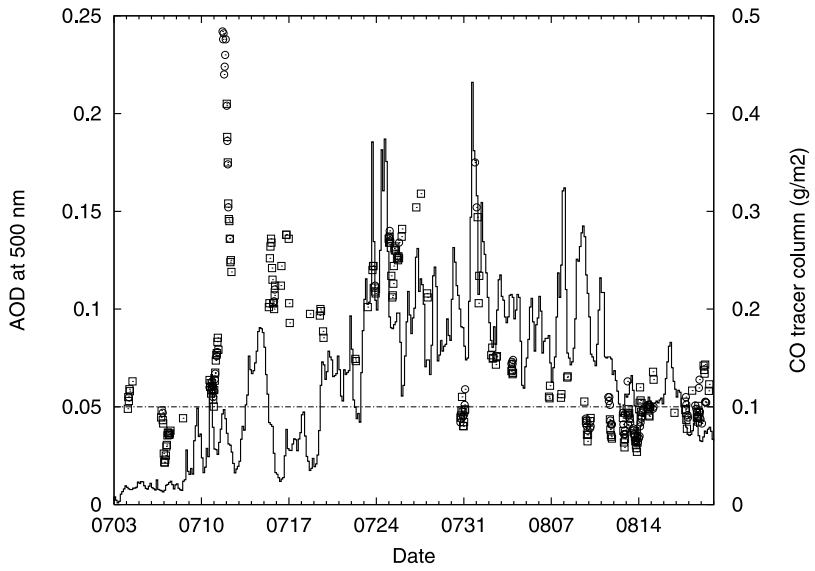

Figure 15. Comparison of hourly mean AOD data at 500 nm for Ny Ålesund from the SP1A instrument (squares) and the PFR instrument (circles), and FLEXPART CO tracer columns above Ny Ålesund (solid line), for 3 July til 19 August 2004. The horizontal dashed line indicates typical background AOD at Ny Ålesund.

streams merged) over the Atlantic. Further back in time, the PES is spread out over a very large region, indicating mixing of different air masses. However, the PES values over anthropogenic source regions are low, with largest anthropogenic CO PSCs from Scotland (not shown). The PES values over the fire region are not particularly high but sufficient for the fire CO PSCs to be larger than anthropogenic ones.

[45] An interesting question is why σ_{ap} values were strongly enhanced from 25 to 28 July but not so much during the following two weeks when CO was still anomalously high. For the period 25–28 July, air parcels descended during the last few days of transport and likely had no contact with the marine boundary layer. Later, in contrast, the air travelled below the station altitude for the last few days and ascended before arrival. This is confirmed by archived video images from the station, which show sunny conditions during the 25–28 July episode but mostly clouds, sometimes at the station level, and rain during the following two weeks. It is, thus, suggested that precipitation during the ascent (and, possibly, deposition in the marine boundary layer) removed a large fraction of the aerosols after the 25–28 episode.

[46] Conditions for AOD measurements at Ny Ålesund are poor in summer because of frequent cloud cover. Despite the data gaps, the smoke aloft is reflected in enhanced AOD values in July and August, particularly during the episode on 24–28 July that was also observed at Zeppelin (Figure 15), and on 1 August. The AOD values are much higher than normally measured background values in summer and are, in fact, comparable to the most severe Arctic Haze episodes observed during the years 2004–2006. Measurements by a micropulse lidar of the Japanese National Institute of Polar Research (see http://mplnet.gsfc.nasa.gov/) in Ny Ålesund show multiple aerosol layers throughout the depth of the troposphere on 11–12 July, 23–25 July, 31 July, and 3 August. On most other days during the presence of the forest fire plumes, the lidar beam could not penetrate low-level clouds.

4. A Possible Effect on Snow Albedo

[47] Since it is known that light absorbing particles immersed in snow can strongly reduce the snow's albedo [*Clarke and Noone*, 1985; *Warren and Wiscombe*, 1981; *Hansen and Nazarenko*, 2004], it seems possible that the boreal forest fire plumes have had a measurable effect on the albedo of Arctic snow and ice. However, because of generally large albedo variability and lack of data such an effect is difficult to prove. We use the radiation measurements at Summit to explore possible effects on the albedo because the temperatures at Summit remained well below freezing, thus limiting the otherwise dominating effect of snow melt on the albedo. During the first major episode at Summit (16–20 July), the BC concentrations were of the order of 300 ng m^{-3}. Assuming a relatively large deposition velocity of 1 mm s^{-1} for the submicrometer BC particles (A. Petzold et al., unpublished manuscript, 2006), about 130 μg m^{-2} BC would have been deposited on the snow over the 5 day period. Considering the calculations of *Warren and Wiscombe* [1981], this is an amount that could produce an observable albedo decrease, especially since the particles would have been deposited directly at the snow surface where they would decrease the albedo most strongly [*Grenfell et al.*, 2002]. Furthermore, of the submicrometer BC particles the smallest ones would have been favored in the dry deposition process, and these small particles are the most effective in decreasing the albedo [*Warren and Wiscombe*, 1981].

[48] Before analyzing the albedo data, we need to take into account the effect of clouds on the albedo. As the attenuation of shortwave radiation by clouds is stronger at longer wavelengths, the spectral composition of the global radiation is shifted toward shorter wavelengths under over-

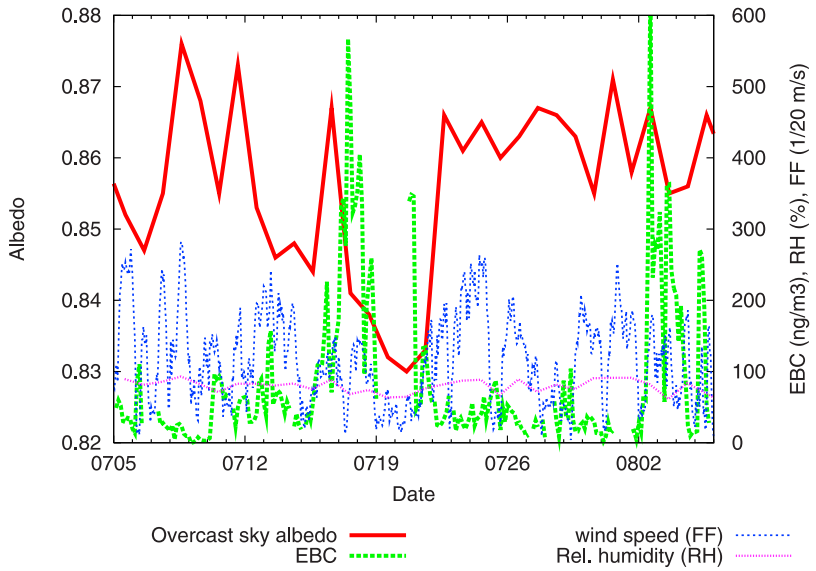

Figure 16. Time series of daily mean overcast sky albedo (red line), EBC (green line), wind speed (blue line), and daily minimum relative humidity (pink line) at Summit, for the period 5 July til 5 August 2004.

cast skies. Since the spectral reflectivity of snow is higher for shorter wavelengths than for longer ones [*Grenfell et al.*, 1981], its broadband albedo is, thus, higher under cloudy conditions. Under overcast (clear) skies, the albedo at Summit is typically 0.86 (0.82). Thus, to better resolve possible changes in snow albedo due to aerosol deposition, a correction is introduced: The ratio between the daily means of direct solar flux (D) and the shortwave flux at the top of the atmosphere (TOA) is used as an indicator for cloud conditions. A linear relationship between this ratio (D/TOA) and albedo (a) ($a = 0.8591 - 0.0474 * D/TOA$) with an explained variance of 39% is found from a fit through all daily observations when global radiation exceeded 200 W m^{-2}. Using this relationship, we calculated a theoretical overcast (oc) sky albedo a_{oc} to remove the cloud cover effect on albedo. Changes in a_{oc} will indicate the influence of other processes that alter the reflectivity of the snow, such as precipitation or, possibly, the deposition of light absorbing aerosols.

[49] The a_{oc} time series shows a pronounced drop of a_{oc} values during the first major EBC event but no clear decrease during the second (Figure 16). Also, values of a_{oc} increase soon after the passage of the first EBC plume. It should be noted that the a_{oc} drop is also present in the uncorrected albedo data but as the correction reduces the data variability, it stands out more clearly after the correction. While the decrease of a_{oc} values during the first episode is suggestive of an influence of aerosol deposition, the subsequent increase, as well as the absence of a clear signal during the second episode show that other factors must also be taken into account. Deposition of fresh snow after the first episode would explain an increase of a_{oc} values, since fresh snow has a higher albedo than aged snow [*Grenfell et al.*, 1981]. While no daily measurements of snowfall are made at Summit, weekly observations showed a 2 cm increase between 21 and 28 July. Archived webcam images of the camp environment suggest the accumulation of fresh snow occurred on 22 and 23 July. Furthermore, daily minimum relative humidity values were 82% on 22 July, substantially more than on the previous days (see Figure 16). An alternative explanation for the albedo recovery is snow drift. Wind speeds were low from 18 July to 20 July (mostly below 2 m s^{-1}) but increased substantially on 21 July to a value of 8.6 m s^{-1} at 2200 UTC (see Figure 16). On 22 July winds remained above 5 m s^{-1} and peaked at 9.8 m s^{-1}. The following days were even more windy. One of the authors (S. W. Hoch) observed that at Summit slight snow drift can occur already at 5 m s^{-1} and wind speeds greater than 7 m s^{-1} always lead to snow drift. Thus, after the EBC episode, the deposited aerosols may have been covered by drifting snow or collected in patches. Discolored, polluted snow patches were recently documented under windy conditions during an extreme pollution event at Spitsbergen [*Stohl et al.*, 2006] by one of the authors (J. Burkhart), and while the discoloration is unlikely at Summit, it is possible that polluted snow may become "patched" during drifting. Wind speeds during the second and less strong EBC episode were generally higher than during the first one and peaked at above 9 m s^{-1} when a_{oc} values increased on 4 August. Thus snow drift was likely during this episode. The archived images of the camp environment also suggest there might have been accumulation of fresh snow on 4 August when also the relative humidity increased.

[50] In summary, we cannot prove that the significant drop in albedo during the first episode was indeed caused by deposition of light absorbing aerosols but we argue that this is a likely explanation. The subsequent recovery and the lack of a similarly strong signal during the second, albeit weaker, EBC episode can be explained by snow drift and the possibility of the accumulation of fresh snow. Both effects would have removed the aerosols from the snow surface where they are most effective [*Grenfell et al.*, 2002]. However, smaller effects on the albedo could persist since decreased albedo can also result from BC particles buried at

a few centimeters depth in the snowpack [*Grenfell et al.*, 2002].

5. Conclusions

[51] This paper presented a study of the impact of boreal forest fires burning in North America in summer 2004 on Arctic concentration levels of light absorbing aerosols and on light extinction in the atmosphere. It combined forward and backward simulations with the FLEXPART transport model with light absorption, EBC, AOD and other measurements at the four Arctic sites Barrow, Alert, Summit, and Zeppelin. Albedo data from Summit were also studied. The main findings are as follows:

[52] 1. The FLEXPART model suggested that pollution plumes from the fires were frequently transported into the Arctic, which is confirmed by satellite images showing smoke plumes in the Arctic. Most of the plumes were lifted above the polar dome, whereas their influence at the surface was less pronounced.

[53] 2. AOD measurements at Barrow, Summit and Zeppelin confirmed the presence of many forest fire plumes during July and August 2004. In fact, strong fire influence was continuously present for more than a month, during which few values were measured that are normally considered as typical for these remote stations. The spectral dependence of the AOD values is unique and confirms that the aerosols were indeed smoke.

[54] 3. Although the Arctic surface was relatively less affected, at all four Arctic sites forest fire plumes with elevated σ_{ap} values/EBC concentrations were found that represented the highest values of the summer half year. However, except for Summit which was impacted especially strongly, the medians for the summer months were quite normal (Table 1), which probably indicates that fire plumes are important also in other years.

[55] 4. Barrow, about 1000 km away from the fires, was strongly affected by the passage of several plumes, especially in July. During the strongest episode, AOD measurements at 500 nm saturated because of too thick smoke but were estimated at above 4–5 units, unprecedented in the NOAA records. At the same time σ_{ap} values at the surface (maximum 3-hour mean of 32 Mm^{-1}) were greater than the highest values measured during Arctic Haze.

[56] 5. For Alert, located almost 3000 km from the fires, FLEXPART suggested that all but one of the plumes passed aloft or were relatively weak at the surface. However, the same plume that impacted Barrow most strongly, led to 3-hour mean σ_{ap} values of up to 0.6 Mm^{-1} also at Alert.

[57] 6. At Summit, 4000 km from the fires, AOD values were above background during almost 2 months, confirming the FLEXPART prediction that smoke was transported continuously through the atmospheric column over Summit. Maximum AOD values were 0.4–0.5 units. Because of its high elevation, Summit was also strongly affected at the surface during two several-day-long episodes when 3-hour mean EBC concentrations of up to 600 ng m^{-3} were measured.

[58] 7. For Zeppelin, 4000 km away from the fires and located in a part of the Arctic that was relatively little affected by fire plumes, FLEXPART suggested an about 3-week long period with moderately high forest fire tracer concentrations, both at the surface and aloft. CO measurements showed an anomaly of about 20–30 ppb from the normal seasonal cycle during this period. There was also a 4-day period with daily mean $\sigma_{ap} > 0.3$ Mm^{-1}, the strongest episode of the summer half year and comparable in strength to Arctic Haze episodes. Levoglucosan concentrations during this period were elevated, confirming transport of aerosols from biomass burning. During most of the rest of the period the station was in clouds where local removal of aerosols was likely important. During noncloudy periods, when measurements were possible, AOD values were typically 0.2 units (up to 0.35 units) and lidar measurements showed pronounced haze layers throughout the troposphere.

[59] 8. At Summit, the albedo of the snow surface dropped by about 3% during the strongest EBC episode. We cannot prove that this drop is indeed due to the deposition of light absorbing aerosols but it is a very likely explanation.

[60] 9. In summary, this case study has shown that boreal forest fires can have a strong influence on the concentrations of light absorbing aerosols and aerosol optical depths in the Arctic. It also argues for a possible influence on the albedo of Arctic snow surfaces. The summer of 2004 has set a new record for the area burned in Alaska and was also severe in Canada but boreal forest fires are a recurring phenomenon. Similarly large areas burned in North America in other years, and areas burned in Siberia can be much larger, for instance, by more than a factor of 4 in the year 2003. Therefore a concentrated effort employing new measurements, statistical analyses of existing data, and models will be needed to fully characterize the impact of boreal forest fires on Arctic air pollution levels, radiation transmission through the Arctic atmosphere, the albedo, and Arctic climate. Such a coordinated effort will be undertaken during the International Polar Year 2007–2009 as part of the POLARCAT project (see http://zardoz.nilu.no/andreas/POLARCAT/).

[61] **Acknowledgments.** We thank S. A. McKeen and G. Frost for making available their inventory of North American anthropogenic emissions. The Swedish EPA funded the aerosol measurements at Zeppelin. We thank M. Shiobara for the plots of lidar backscatter from Ny Ålesund (http://mplnet.gsfc.nasa.gov/). Two anonymous reviewers have provided valuable comments that helped in revising the original version of this paper.

References

Arnott, W. P., K. Hamasha, H. Moosmüller, P. J. Sheridan, and J. A. Ogren (2005), Towards aerosol light-absorption measurements with a 7-wavelength aethalometer: Evaluation with a photoacoustic instrument and 3-wavelength nephelometer, *Aerosol Sci. Technol.*, *39*, 17–29.

Barrie, L. A. (1986), Arctic air pollution—An overview of current knowledge, *Atmos. Environ.*, *20*, 643–663.

Bond, T. C., and R. W. Bergstrom (2005), Light absorption by carbonaceous particles: An investigative review, *Aerosol Sci. Technol.*, *39*, 1–41.

Bond, T. C., T. L. Anderson, and D. Campbell (1999), Calibration and intercomperison of filter-based measurements of visible light absorption by aerosols, *Aerosol Sci. Technol.*, *30*, 582–600.

Bond, T. C., D. G. Streets, K. F. Yarber, S. M. Nelson, J.-H. Woo, and Z. Klimont (2004), A technology-based global inventory of black and organic carbon emissions from combustion, *J. Geophys. Res.*, *109*, D14203, doi:10.1029/2003JD003697.

Clarke, A. D., and K. J. Noone (1985), Soot in the Arctic snowpack: A cause for perturbations in radiative transfer, *Atmos. Environ.*, *19*, 2045–2053.

Damoah, R., N. Spichtinger, C. Forster, P. James, I. Mattis, U. Wandinger, S. Beirle, and A. Stohl (2004), Around the world in 17 days—Hemispheric-scale transport of forest fire smoke from Russia in May 2003, *Atmos. Chem. Phys.*, *4*, 1311–1321.

Damoah, R., N. Spichtinger, R. Servranckx, M. Fromm, E. W. Eloranta, I. A. Razenkov, P. James, M. Shulski, C. Forster, and A. Stohl (2006), Transport modelling of a pyro-convection event in Alaska, *Atmos. Chem. Phys.*, *5*, 173–185.

de Gouw, J. A., et al. (2006), Volatile organic compounds composition of merged and aged forest fire plumes from Alaska and western Canada, *J. Geophys. Res.*, *111*, D10303, doi:10.1029/2005JD006175.

Delene, D. J., and J. A. Ogren (2002), Variability of aerosol optical properties at four North American surface monitoring sites, *J. Atmos. Sci.*, *59*, 1135–1150.

Dye, C., and K. E. Yttri (2005), Determination of monosaccharide anhydrides in atmospheric aerosols by use of high-resolution mass spectrometry combined with high performance liquid chromatography, *Anal. Chem.*, *77*, 1853–1858.

Eckhardt, S., A. Stohl, H. Wernli, P. James, C. Forster, and N. Spichtinger (2004), A 15-year climatology of warm conveyor belts, *J. Clim.*, *17*, 218–237.

Emanuel, K. A., and M. Živković-Rothman (1999), Development and evaluation of a convection scheme for use in climate models, *J. Atmos. Sci.*, *56*, 1766–1782.

European Center for Medium-Range Weather Forecasts (2002), IFS documentation, edited by P. W. White, Reading, U. K.

Flannigan, M. D., B. J. Stocks, and B. M. Wotton (2000), Climate change and forest fires, *Sci. Total Environ.*, *262*, 221–229.

Forster, C., et al. (2001), Transport of boreal forest fire emissions from Canada to Europe, *J. Geophys. Res.*, *106*, 22,887–22,906.

Forster, C., A. Stohl, and P. Seibert (2006), Parameterization of convective transport in a Lagrangian particle dispersion model and its evaluation, *J. Appl. Meteorol.*, in press.

Francey, R. J., et al. (1996), Global Atmospheric Sampling Laboratory (GASLAB): Supporting and extending the Cape Grim trace gas programs, in *Baseline Atmospheric Program (Australia) 1993*, edited by R. J. Francey, A. L. Dick, and N. Derek, pp. 8–29, Bur. of Meteorol. and CSIRO Div. of Atmos. Res., Melbourne, Vic., Australia.

Fraser, M. P., and K. Lakshmanan (2000), Using levoglucosan as a molecular marker for the long-range transport of biomass combustion aerosols, *Environ. Sci. Technol.*, *34*, 4560–4564.

French, N. H. F., E. S. Kasischke, and D. G. Williams (2003), Variability in the emission of carbon-based trace gases from wildfire in the Alaskan boreal forest, *J. Geophys. Res.*, *108*(D1), 8151, doi:10.1029/2001JD000480.

Frost, G. J., S. A. McKeen, M. Trainer, T. B. Ryerson, and J. A. Neuman, et al. (2006), Effects of changing power plant NOx emissions on ozone in the eastern United States: Proof of concept, *J. Geophys. Res.*, *111*, D12306, doi:10.1029/2005JD006354.

Grenfell, T. C., D. K. Perovich, and J. A. Ogren (1981), Spectral albedos of an alpine snowpack, *Cold Reg. Sci. Technol.*, *4*, 121–127.

Grenfell, T. C., B. Light, and M. Sturm (2002), Spatial distribution and radiative effects of soot in the snow and sea ice during the SHEBA experiment, *J. Geophys. Res.*, *107*(C10), 8032, doi:10.1029/2000JC000414.

Hansen, J., and L. Nazarenko (2004), Soot climate forcing via snow and ice albedos, *Proc. Natl. Acad. Sci. U.S.A.*, *101*, 423–428, doi:10.1073/pnas.2237157100.

Herber, A., L. W. Thomason, H. Gernandt, U. Leiterer, D. Nagel, K.-H. Schulz, J. Kaptur, T. Albrecht, and J. Notholt (2002), Continuous day and night aerosol optical depth observations in the Arctic between 1991 and 1999, *J. Geophys. Res.*, *107*(D10), 4097, doi:10.1029/2001JD000536.

Hermansen, O., N. Schmidbauer, C. Lunder, F. Stordal, J. Schaug, C. Wehrli, I. T. Pedersen, K. Holmén, O.-A. Braathen, and J. Ström (2005), Greenhouse gas monitoring at the Zeppelin station, Ny-Alesund, Svalbard, Norway, annual report 2004, *Rep. NILU OR 33/2005*, Norw. Inst. for Air Res., Kjeller, Norway.

Hsu, N. C., J. R. Herman, J. F. Gleason, O. Torres, and C. J. Seftor (1999), Satellite detection of smoke aerosols over a snow/ice surface by TOMS, *Geophys. Res. Lett.*, *26*, 1165–1168.

Kasischke, E. S., E. J. Hyer, P. C. Novelli, L. P. Bruhwiler, N. H. F. French, A. I. Sukhinin, J. H. Hewson, and B. J. Stocks (2005), Influences of boreal fire emissions on Northern Hemisphere atmospheric carbon and carbon monoxide, *Global Biogeochem. Cycles*, *19*, GB1012, doi:10.1029/2004GB002300.

Kim, Y., H. Hatsushika, R. R. Muskett, and K. Yamazaki (2005), Possible effect of boreal wildfire soot on Arctic sea ice and Alaska glaciers, *Atmos. Environ*, *39*, 3513–3520.

Klonecki, A., P. Hess, L. Emmons, L. Smith, J. Orlando, and D. Blake (2003), Seasonal changes in the transport of pollutants into the Arctic troposphere-model study, *J. Geophys. Res.*, *108*(D4), 8367, doi:10.1029/2002JD002199.

Koch, D., and J. Hansen (2005), Distant origins of Arctic black carbon: A Goddard Institute for Space Studies ModelE experiment, *J. Geophys. Res.*, *110*, D04204, doi:10.1029/2004JD005296.

Langenfelds, R. L., L. P. Steele, L. N. Cooper, D. A. Spencer, D. M. Etheridge, and M. P. Lucarelli (1999), CSIRO GASLAB measurement of CO_2, CH_4, CO, H_2 and N_2O by gas chromatography, technical report, CSIRO Mar. and Atmos. Res., Hobart, Tas., Australia.

Lavoué, D. (2000), Transport to the Arctic region of carbon aerosols emitted by biomass burning in boreal and temperate regions (Transport vers la région arctique de l'aérosol carboné émis par les feux de biomasse des régions boréale et tempérée), Ph.D. thesis, Univ. of Paris VII, Paris.

Lavoué, D., C. Liousse, H. Cachier, B. J. Stocks, and J. G. Goldammer (2000), Modeling of carbonaceous particles emitted by boreal and temperate wildfires at northern latitudes, *J. Geophys. Res.*, *105*, 26,871–26,890.

Liu, X., J. E. Penner, and M. Herzog (2005), Global modeling of aerosol dynamics: Model description, evaluation, and interactions between sulfate and nonsulfate aerosols, *J. Geophys. Res.*, *110*, D18206, doi:10.1029/2004JD005674.

McArthur, L. J. B. (1998), Baseline Surface Radiation Network BSRN, operations manual, *WMO/TD 879*, World Clim. Res. Programme, World Meteorol. Organ., Geneva, Switzerland.

Novelli, P. C., K. A. Masarie, P. M. Lang, B. D. Hall, R. C. Myers, and J. W. Elkins (2003), Reanalysis of tropospheric CO trends: Effects of the 1997–1998 wildfires, *J. Geophys. Res.*, *108*(D15), 4464, doi:10.1029/2002JD003031.

Olivier, J. G. J., and J. J. M. Berdowski (2001), Global emissions sources and sinks, in *The Climate System*, edited by J. Berdowski, R. Guicherit, and B. J. Heij, pp. 33–78, A. A. Balkema, Brookfield, Vt.

Park, R. J., et al. (2005), Export efficiency of black carbon aerosol in continental outflow: Global implications, *J. Geophys. Res.*, *110*, D11205, doi:10.1029/2004JD005432.

Pfister, G., P. G. Hess, L. K. Emmons, J.-F. Lamarque, C. Wiedinmyer, D. P. Edwards, G. Petron, J. C. Gille, and G. W. Sachse (2005), Quantifying CO emissions from the 2004 Alaskan wildfires using MOPITT CO data, *Geophys. Res. Lett.*, *32*, L11809, doi:10.1029/2005GL022995.

Porch, W. M. (1989), Blue moons and large fires, *Appl. Opt.*, *28*, 1778–1784.

Robock, A. (1991), Surface cooling due to forest fire smoke, *J. Geophys. Res.*, *96*, 20,869–20,878.

Scholnik, G., and Y. Rudich (2006), Detection of levoglucosan in atmospheric aerosols: A review, *Anal. Bioanal. Chem.*, *385*, 26–33.

Seibert, P., and A. Frank (2004), Source-receptor matrix calculation with a Lagrangian particle dispersion model in backward mode, *Atmos. Chem. Phys.*, *4*, 51–63.

Sharma, S., D. Lavoué, H. Cachier, L. A. Barrie, and S. L. Gong (2004), Long-term trends of the black carbon concentrations in the Canadian Arctic, *J. Geophys. Res.*, *109*, D15203, doi:10.1029/2003JD004331.

Shaw, G. E. (1995), The Arctic Haze phenomenon, *Bull. Am. Meteorol. Soc.*, *76*, 2403–2412.

Sheridan, P. J., et al. (2005), The Reno Aerosol Optics Study: An evaluation of aerosol absorption measurement methods, *Aerosol Sci. Technol.*, *39*, 1–16.

Shipham, M. C., A. S. Bachmeier, D. R. Cahoon Jr., and E. V. Browell (1992), Meteorological overview of the Arctic Boundary Layer Expedition (ABLE 3A) flight series, *J. Geophys. Res.*, *97*, 16,395–16,419.

Simoneit, B. R. T., J. J. Schauer, C. G. Nolte, D. R. Oros, V. O. Elias, M. P. Fraser, W. F. Rogge, and G. R. Cass (1999), Levoglucosan, a tracer for cellulose in biomass burning and atmospheric particles, *Atmos. Environ.*, *33*, 173–182.

Spichtinger, N., M. Wenig, P. James, T. Wagner, U. Platt, and A. Stohl (2001), Satellite detection of a continental-scale plume of nitrogen oxides from boreal forest fires, *Geophys. Res. Lett.*, *28*, 4579–4582.

Spichtinger, N., R. Damoah, S. Eckhardt, C. Forster, P. James, S. Beirle, T. Marbach, T. Wagner, P. C. Novelli, and A. Stohl (2004), Boreal forest fires in 1997 and 1998: A seasonal comparison using transport model simulations and measurement data, *Atmos. Chem. Phys.*, *4*, 1857–1868.

Stocks, B. J., et al. (2003), Large forest fires in Canada, 1959–1997, *J. Geophys. Res.*, *108*(D1), 8149, doi:10.1029/2001JD000484.

Stohl, A. (2006), Characteristics of atmospheric transport into the Arctic troposphere, *J. Geophys. Res.*, *111*, D11306, doi:10.1029/2005JD006888.

Stohl, A., and D. J. Thomson (1999), A density correction for Lagrangian particle dispersion models, *Boundary Layer Meteorol.*, *90*, 155–167.

Stohl, A., M. Hittenberger, and G. Wotawa (1998), Validation of the Lagrangian particle dispersion model FLEXPART against large scale tracer experiment data, *Atmos. Environ.*, *32*, 4245–4264.

Stohl, A., C. Forster, S. Eckhardt, N. Spichtinger, H. Huntrieser, J. Heland, H. Schlager, S. Wilhelm, F. Arnold, and O. Cooper (2003), A backward modeling study of intercontinental pollution transport using aircraft measurements, *J. Geophys. Res.*, *108*(D12), 4370, doi:10.1029/2002JD002862.

Stohl, A., C. Forster, A. Frank, P. Seibert, and G. Wotawa (2005), Technical note: The Lagrangian particle dispersion model FLEXPART version 6.2, *Atmos. Chem. Phys.*, *5*, 2461–2474.

Stohl, A., et al. (2006), Arctic smoke—Record high air pollution levels in the European Arctic due to agricultural fires in eastern Europe, *Atmos. Chem. Phys. Disc.*, *6*, 9655–9722.

Stone, R. S. (2002), Monitoring aerosol optical depth at Barrow, Alaska and South Pole; Historical overview, recent results, and future goals, in *Proceedings of the 9th Workshop Italian Research on Antarctic Atmosphere, Rome, Italy, 22–24 October 2001*, edited by M. Colacino, pp. 123–144, Ital. Phys. Soc., Bologna, Italy.

Van de Hulst, H. C. (1957), *Light Scattering by Small Particles*, 422 pp., John Wiley, Hoboken, N. J.

Warneke, C., et al. (2006), Biomass burning and anthropogenic sources of CO over New England in the summer 2004, *J. Geophys. Res.*, *111*, D23S15, doi:10.1029/2005JD006878.

Warren, S. G., and W. J. Wiscombe (1981), A model for the spectral albedo of snow. II: Snow containing amtospheric aerosols, *J. Atmos. Sci.*, *37*, 2734–2745.

Wehrli, C. (2005), GAWPFR: A Network of Aerosol Optical Depth Observations with Precision Filter Radiometers, in *WMO/GAW Experts Workshop on a Global Surface-based Network for Long Term Observations of Column Aerosol Optical Properties, GAW Rep. 162, WMO TD 1287*, pp. 36–39, World Meteorol. Organ., Geneva, Switzerland.

Weingartner, E., H. Saathoff, M. Schnaiter, N. Streit, B. Bitnar, and U. Baltensberger (2003), Absortpion of light by soot particles: Determination of the absorption coefficient by means of aethalometers, *Aerosol Sci.*, *34*, 1445–1463.

Wotawa, G., P. C. Novelli, M. Trainer, and C. Granier (2001), Interannual variability of summertime CO concentrations in the Northern Hemisphere explained by boreal forest fires in North America and Russia, *Geophys. Res. Lett.*, *28*, 4575–4578.

E. Andrews, T. Mefford, J. A. Ogren, and R. Stone, Global Monitoring Division, Earth System Research Laboratory, NOAA, Boulder, CO 80305, USA.

J. F. Burkhart, School of Engineering, University of California, Merced, CA 95344, USA.

C. Forster, C. Lunder, K. Stebel, A. Stohl, K. Tørseth, and K. E. Yttri, Norwegian Institute for Air Research, Instituttveien 18, N-2027 Kjeller, Norway. (ast@nilu.no)

A. Herber, Alfred Wegener Institute, D-27515 Bremerhaven, Germany.

S. W. Hoch, Institute for Atmospheric and Climate Science, Eidgenössische Technische Hochschule, CH-8092 Zurich, Switzerland.

D. Kowal, National Geophysical Data Center, NOAA, Boulder, CO 80305, USA.

S. Sharma, Environment Canada, 4905 Dufferin Street, Toronto, ON, Canada M3H5T4.

N. Spichtinger, Wissenschaftszentrum Weihenstephan, Technical University of Munich, DE-80333 Munich, Germany.

J. Ström, Department of Applied Environmental Science, Stockholm University, SE-10691 Stockholm, Sweden.

C. Wehrli, Physical-Meteorological Observatory, CH-7260 Davos, Switzerland.